Available online at www.sciencedirect.com
SCIENCE DIRECT®
Biochemical Pharmacology 67 (2004) 2141–2165
Biochemical Pharmacology
www.elsevier.com/locate/biochempharm

Inverse gene expression patterns for macrophage activating hepatotoxicants and peroxisome proliferators in rat liver

Michael McMillian[a,*], Alex Y. Nie[a], J. Brandon Parker[a], Angelique Leone[a], Michael Kemmerer[a], Stewart Bryant[a], Judy Herlich[a], Lynn Yieh[b], Anton Bittner[b], Xuejun Liu[b], Jackson Wan[b], Mark D. Johnson[a]

[a]*Johnson & Johnson Pharmaceutical Research & Development, LLC, Raritan, NJ, USA*
[b]*Johnson & Johnson Pharmaceutical Research & Development, LLC, La Jolla, CA, USA*

Received 16 October 2003; accepted 28 January 2004

Abstract

Macrophage activation contributes to adverse effects produced by a number of hepatotoxic compounds. Transcriptional profiles elicited by two macrophage activators, LPS and zymosan A, were compared to those produced by 100 paradigm compounds (mostly hepatotoxicants) using cDNA microarrays. Several hepatotoxicants previously reported to activate liver macrophages produced transcriptional responses similar to LPS and zymosan, and these were used to construct a gene signature profile for macrophage activators in the liver. Measurement of cytokine mRNAs in the same liver samples by RT–PCR independently confirmed that these compounds are associated with macrophage activation. In addition to expected effects on acute phase proteins and metabolic pathways that are regulated by LPS and inflammation, a strong induction was observed for many endoplasmic reticulum-associated stress/chaperone proteins. Additionally, many genes in our macrophage activator signature profile were well-characterized PPARα-induced genes which were repressed by macrophage activators. A shared gene signature profile for peroxisome proliferators was determined using a training set of clofibrate, WY 14643, diethylhexylphthalate, diisononylphthalate, perfluorodecanoic acid, perfluoroheptanoic acid, and perfluorooctanoic acid. The signature profile included macrophage activator-induced genes that were repressed by peroxisome proliferators. NSAIDs comprised an interesting pharmacological class in that some compounds, notably diflunisal, co-clustered with peroxisome proliferators whereas several others co-clustered with macrophage activators, possibly due to endotoxin exposure secondary to their adverse effects on the gastrointestinal system. While much of these data confirmed findings from the literature, the transcriptional patterns detected using this toxicogenomics approach showed relationships between genes and biological pathways requiring complex analysis to be discerned.

Keywords: Microarray; Kupffer cells; Macrophage; LPS; Peroxisome proliferator; ER stress

1. Introduction

Transcriptional profiling for toxicity assessment, i.e. toxicogenomics, offers a relatively simple technological platform for use in drug safety evaluation, including mechanistic toxicity studies and preemptive screening for potential adverse effects [1–3]. The ability to simultaneously measure thousands of gene responses is rapidly increasing our understanding of cellular responses to toxicants, and will enable the identification of useful mRNA biomarkers for many different pathologies, possibly allowing earlier detection before traditional microscopic effects become apparent. The experimental approaches that various groups have taken in applying toxicogenomics vary dramatically. Currently there is no standardized method for designing and interpreting toxicology experiments using microarrays. Toxicogenomics is a novel application of an emerging technology, and there are little data available in the public domain . Therefore, it is important to apply a variety of strategies to fully explore the potential uses of mRNA measurements and to determine the best approaches

Abbreviations: ANIT, 1-naphthyl isothiocyanate; LPS, lipopolysaccharide; NSAID, nonsteroidal anti-inflammatory drugs; TNFα, tumor necrosis factor alpha; IL-1, interleukin-1; IL-6, interleukin-6; iNOS, inducible nitric oxide synthase; RT–PCR, reverse transcription polymerase chain reaction; cDNA, complementary DNA

* Corresponding author. Tel.: +1-908-2187235; fax: +1-908-2180668.
E-mail address: mmcmilli@prdus.jnj.com (M. McMillian).

0006-2952/$ – see front matter © 2004 Elsevier Inc. All rights reserved.
doi:10.1016/j.bcp.2004.01.029

in a toxicology setting. Many groups have chosen to investigate a small number of compounds in depth at multiple doses, multiple times, and in multiple tissues [4–7]. Gene signature profiles that distinguish different classes of toxicants are a priority, especially for groups involved in pharmaceutical development. Most of the toxicogenomics effort has been directed toward validating observed gene changes, 'phenotypically anchoring' them to consequent histopathological changes [7]. Since false positives are an expected result with so many parallel gene expression measurements, several groups have chosen to emphasize pathways populated by positive genes rather than individual gene changes.

A broad coverage approach to toxicogenomics was undertaken by including multiple representatives of each toxicity class to detect overlapping gene expression signals. Paradigm compounds were chosen based on well-studied toxicities in rat liver to obviate the need for histopathology; as it was difficult to justify extensive in-life studies on 100 known hepatotoxicants. In our experience, high doses of toxicants were generally required to obtain meaningful and robust gene changes in the liver; so the approximate maximally tolerated doses were used from the literature for these studies. Changes in gene expression were usually observed at our chosen timepoint of 24 h after a single dose of hepatotoxicant, which preceded and presaged most histopathological endpoints.

In the present study, cDNA microarrays were used to characterize macrophage (particularly liver macrophage = Kupffer cell) induced hepatotoxicity. In addition to experimental activators such as LPS and zymosan A, Kupffer cells are activated by many drugs and solvents, either directly or by stimulation of endotoxin absorption from the gut. Activated Kupffer cells contribute to hepatotoxicity by producing free radicals (including superoxide and nitric oxide) and cytokines—particularly TNFα, IL-1, and IL-6. TNFα and, to a lesser extent IL-1, are major mediators of cytotoxicity, and IL-6 is the major regulator of the acute phase response [8–11]. Activated Kupffer cells also release chemokines, which attract and activate neutrophils and lymphocytes that can potentiate hepatotoxicity [8]. Even at subtoxic doses macrophage activators can dramatically affect liver function. For example, macrophage activation leads to a robust downregulation of xenobiotic-handling pathways in the liver, including many cytochromes P450 and transporter proteins [12,13].

The acute phase response is also sensitive to macrophage activation, resulting in a profoundly altered profile of secreted blood proteins from liver that is important in fighting infection and healing wounds [11]. One group has reported that beagle dogs incurred acute phase responses in about half of their single dose toxicity studies, suggesting that Kupffer cell activation is a common response to compounds in this species [14]. A number of hepatotoxicants are also reportedly macrophage activators in the rat, and a macrophage activator gene signature profile will prove useful in detecting drug candidates with this activity.

LPS and zymosan A are particularly robust stimuli that elicit a large number and magnitude of hepatic gene expression changes on our microarray. This allows for extensive comparisons between these two experimental macrophage activators and other compounds, as well as gene pathways involved in their responses. The present studies provide new information about potential modes of action of several prototypical hepatic toxicants and provide a gene signature set that can be used to monitor liver responses to macrophage activation. Additionally, a strong physiological antagonism is observed at the gene level between macrophage activators and PPARα agonists in rat liver, similar to that reported between inflammatory stimuli and PPARγ agonists in several other tissues [15].

2. Materials and methods

2.1. Compounds

All compounds were of the highest grade obtainable from Sigma-Aldrich (St. Louis, MO), except troglitazone and WY 14643 were from Biomol (Plymouth Meeting, PA).

2.2. In vivo studies

The rat is often used as a test species for preclinical toxicology studies during pharmaceutical development, and abundant literature exists for effects of a variety of toxic compounds in this species. Healthy male, 7-week-old Sprague–Dawley rats of about 275 g body weight (Charles River Laboratories, Inc.) were used for these studies. The animals were individually housed, on a 12 h light/dark cycle, and fed Purina Rodent Chow ad libitum. Rats were weighed, numbered on their tails, and inspected (unhealthy or small-forage animals were removed from the study) on the day prior to dosing. Rats were dosed at 3–5 min intervals to allow exsanguination (severing vena cava and aorta under CO_2 analgesia) and necropsy at exactly 24 h for all compounds. Rats were fasted after dosing until necropsy the following morning. Doses were selected as a high toxic dose from Merck Index and/or literature references, and are given in Appendix A; 5 g/kg was chosen as an upper limit dose. At low and often even at moderately high doses, most compounds produced few gene changes by our microarray technology. Even at high, reportedly toxic doses, many compounds produced minimal gene changes (less than 10 gene changes of twofold or more), and their doses were increased or the route of administration changed to increase gene responses. For example, valproic acid (600 mg/kg) was increased to 1000 mg/kg. Tetracycline (500 mg/kg p.o.) was changed to 600 mg/kg i.p. Niacin (2 g/kg) was increased to 5 g/kg. Rotenone (6 mg/kg i.p.)

was increased to 100 mg/kg p.o. Several compounds produced minimal gene changes in liver even at the highest dose examined and were essentially indistinguishable from vehicle treatments or untreated control samples: quercetin (4 g/kg), amiodarone (1 g/kg), troglitazone (500 mg/kg), paraquat (100 mg/kg), famotidine (500 mg/kg), metformin (750 mg/kg), gabapentin (3000 mg/kg), and glycine (500 mg/kg i.p.). In all instances, the animals were humanely handled in accordance to IACUC guidelines.

2.3. RNA isolation

The livers were removed and an approximately 200 mg strip from the medial lobe was snap-frozen in liquid nitrogen. We routinely use sections from the medial lobe of the liver to assess histopathology in 5-day toxicology studies, hence, the same region was chosen for toxicogenomics studies. Liver samples were stored at −70 °C until RNA extraction. Total RNA was extracted using Qiagen RNEasy Midi kits (Qiagen, Inc. Valencia, CA) as per kit instructions. The amount of RNA in the samples was determined spectrophotometrically by absorbance ratio at 260 and 280 nm. Quality of RNA in the samples was assessed using rRNA peaks determined by an Agilent 2100 Bioanalyzer.

RNA and probe preparation for microarray analysis—one round of T7 polymerase-based linear RNA amplification was performed by reverse transcription of RNA with a T7 promoter oligo(dT) primer. Cy3-dCTP labeled fluorescent cDNA probe was synthesized from the amplified RNA as described [16]. Probes were then purified with a PCR purification kit (Qiagen, Inc.), vacuum-dried, and resuspended in 55 μl of hybridization buffer (Version 2 hybridization buffer, Amersham Pharmacia Biotech, Piscataway, NJ, with 50% formamide) containing rat Cot1 DNA (Applied Genetics Laboratories, Melbourne, FL).

2.4. Microarrays

cDNA clones printed on the microarrays were obtained from Research Genetics (IMAGE consortium) and were verified by DNA sequencing. The clones were PCR amplified and purified with a PCRQuick purification kit (Qiagen, Inc.), then mixed 1:1 with a 10 M NaSCN printing buffer. A contact pin microarrayer (Generation III Array Spotter, Molecular Dynamics) was used to spot the clones in duplicate on amino silane-coated slides (Corning). Each slide contained two identical panels of 3434 gene spots (detailed at http://www.mimicell.com/lps/). Printed glass slides were incubated for 10 min at room temperature in isopropanol. The treated slides were rinsed with deionized water and dried by centrifugation.

The probes were denatured at 95 °C for 2 min, placed at room temperature for 5 min, and then applied to the slides. The slides were covered with glass coverslips, sealed with DPX (Fluka) and hybridized at 42 °C overnight. After hybridization, the slides were submerged in 2× SSC, 0.2% SDS at 42 °C and the cover slips were removed. Wash conditions consisted of the following steps: 1× SSC, 0.2% SDS at 42 °C for 5 min; 0.1× SSC, 0.2% SDS at 42 °C for 5 min; 0.1× SSC at room temperature for 1 min. The slides were dried by centrifugation and scanned with a confocal laser scanner (Array Scanner, Molecular Dynamics). Intensity values for each spot of the array were obtained using Autogene software (BioDiscovery).

2.5. Data normalization

Each labeled RNA sample was hybridized to two microarray slides. Since each microarray slide contained two panels of 3434 genes, expression of each gene was determined from the Cy3 intensities of four spots. Spline normalization was applied to the raw intensities (log values) across the four panels from the same RNA sample. The mean of log intensities was then calculated for each gene on the array after all the outlier spots were removed. A spot was regarded as an outlier and removed whenever its intensity value was >1.4 or <0.7 times of the mean for that gene.

All microarray data from samples hybridized on the same day (up to 24 RNA samples) were Spline normalized after the intensities were sorted by magnitude. For each microarray sample, the intensity data were linear normalized; ranking intensity data from a low of 0 and a high of 1.0, intensities at 0.75 were set equal to 100, and intensities at or below 0.2 were set to 0.2 (background). Outlier samples were defined as those with low Pearson's correlation coefficients ($r < 0.80$) relative to other microarray samples from same day hybridizations and were removed from analysis.

To correct for day-to-day hybridization effects, ratios were determined for each gene for each samples using the geometric mean for that gene from all same-day hybridization microarray samples as divisor. Untreated control and vehicle control data were indistinguishable by cluster analyses and were pooled as reference data. Typically microarray samples for the same compound set were hybridized on three different days; those data were pooled and the geometric mean of all the control microarray samples (untreated, methocel or saline treated from same day hybridizations) was used to determine gene expression ratios relative to control, which were used for data analysis.

2.6. Data analysis

The majority of genes on our internal microarray did not contribute information required to distinguish one specific toxicity class from other classes, and gene selection approaches were necessary to identify the most useful genes for separating one toxicity class from another [17]. A number of gene selection approaches were employed in the present study.

2.6.1. Unsupervised gene selection

Each gene was evaluated for its inter-treatment versus within-treatment variability using ANOVA, and 50–200 genes with the smallest P value ($P < 10^{-10}$) were then selected for either clustering or discriminant analysis.

2.6.2. Discriminant analysis and cross-validation

Discriminant analysis was performed to test the separability between predefined treatment classes. Using Partek™ software (Partek Inc., St. Charles, MI), a 10-fold cross-validation was conducted with linear discriminant functions and proportional prior probabilities. Prior to each iteration in discriminant analysis, 100 genes were selected using a genetic algorithm. The separability of the groups was then represented by the overall accuracy of prediction. In this study, the overall prediction accuracy for macrophage activators was 96.5%.

2.6.3. Selection of predictive genes for a class of treatments

A number of genes were selected to best separate a predefined treatment class from the other treatments. The predefined treatment group had to be validated by cross-validation-enforced discriminant analysis and only those with >90% prediction accuracy could be regarded as valid. This process was also aided by the Partek™ software. Genes were searched with a forward-selection method and stopped when a perfect separation was achieved or no significant improvement was observed. At each step, a posterior error was estimated using the linear discriminant analysis.

2.6.4. Selection of responsive genes to a class of treatment and analysis of selected genes

Different from the predictive gene selection discussed above, this selection of genes was a univariate approach in which each gene was evaluated by its variability between the predefined treatment class and the other treatments. The Student's t test was used for this purpose. Genes with the smallest P values were selected as the most responsive genes. To avoid noise from low expression genes that might appear significant, an arbitrary criterion was applied so that only genes with >1.5-fold (i.e. maximum intensity greater than 1.5 times of the minimum intensity) variability across the databases were selected.

2.6.5. Clustering and visualization

Aided by OmniViz Pro™ software version 3.6 (OmniViz Inc., Maynard, MA), microarray samples with all or selected genes were hierarchically clustered using an agglomerative, complete-linkage algorithm and Euclidean distance metric. Compounds and genes were clustered with the same algorithm and organized in a dendrogram tree.

The selected genes were then annotated with gene ontology information aided by the online tool EASE (http://david.niaid.nih.gov/david/ease.htm).

2.7. RT–PCR

Probe and primer sets for several cytokine mRNA markers of macrophage activation—TNFα, IL-1β, IL-6 and iNOS—were obtained as kits from Applied Biosystems (Foster City, CA), and TaqMan assays were performed as per instructions. Confirmatory PCR was not performed on every macrophage activator-regulated gene in liver. However, of the 50 gene expression changes examined by both microarray and PCR, all but two showed excellent qualitative agreement; larger magnitude increases were generally observed by PCR.

3. Results

3.1. Identification of macrophage activator-like compounds

Both LPS and zymosan A were robust genomic stimuli in the liver, with more than 400 genes on the microarray being repressed or induced greater than twofold by each compound. Clustering analysis using all of the genes on the microarray showed that multiple replicates of a number of other compounds co-clustered with LPS and zymosan A (Fig. 1): allyl alcohol (125 mpg), bromobenzene (900 mpg), carbon tetrachloride (3200 mpg), the lymphocyte activator concanavalin A (20 mpg), coumarin (400 mpg), dimethylnitrosamine (50 mpg), the topoisomerase inhibitor etoposide (120 mpg), the macrophage toxin gadolinium chloride (300 mpg), galactosamine (3000 mpg), methylenedianiline (100 mpg), naphthylisothiocyanate (ANIT, 200 mpg), thioacetamide (150 mpg) and a number of NSAIDs—diclofenac (75 mpg), flufenamic acid (250 mpg), fenbufen (250 mpg), and flurbiprofen (40 mpg). Many of these compounds have been reported previously to induce Kupffer cell activation.

A second unsupervised clustering method used only those genes with the highest inter-treatment variability as determined by ANOVA. Fig. 2 shows the clustering analysis using the 50 genes with the smallest P value from ANOVA. Most of the same compounds co-clustered with LPS and zymosan A using the smaller gene set as was observed using all genes. The exceptions were bromobenzene, fenbufen, and the bile duct toxins (ANIT and methylenedianiline), which no longer co-clustered, while hydrazine hydrate (60 mpg), amsacrine (20 mpg), and indomethacin (30 mpg), now co-clustered with LPS and zymosan A.

3.2. Macrophage activator-specific gene expression profiles

A set of 100 genes was selected (using a P value cutoff) that best distinguishes LPS, zymosan, and the above macrophage activator-like compounds (using only co-clustered treatments with at least two replicates common to both

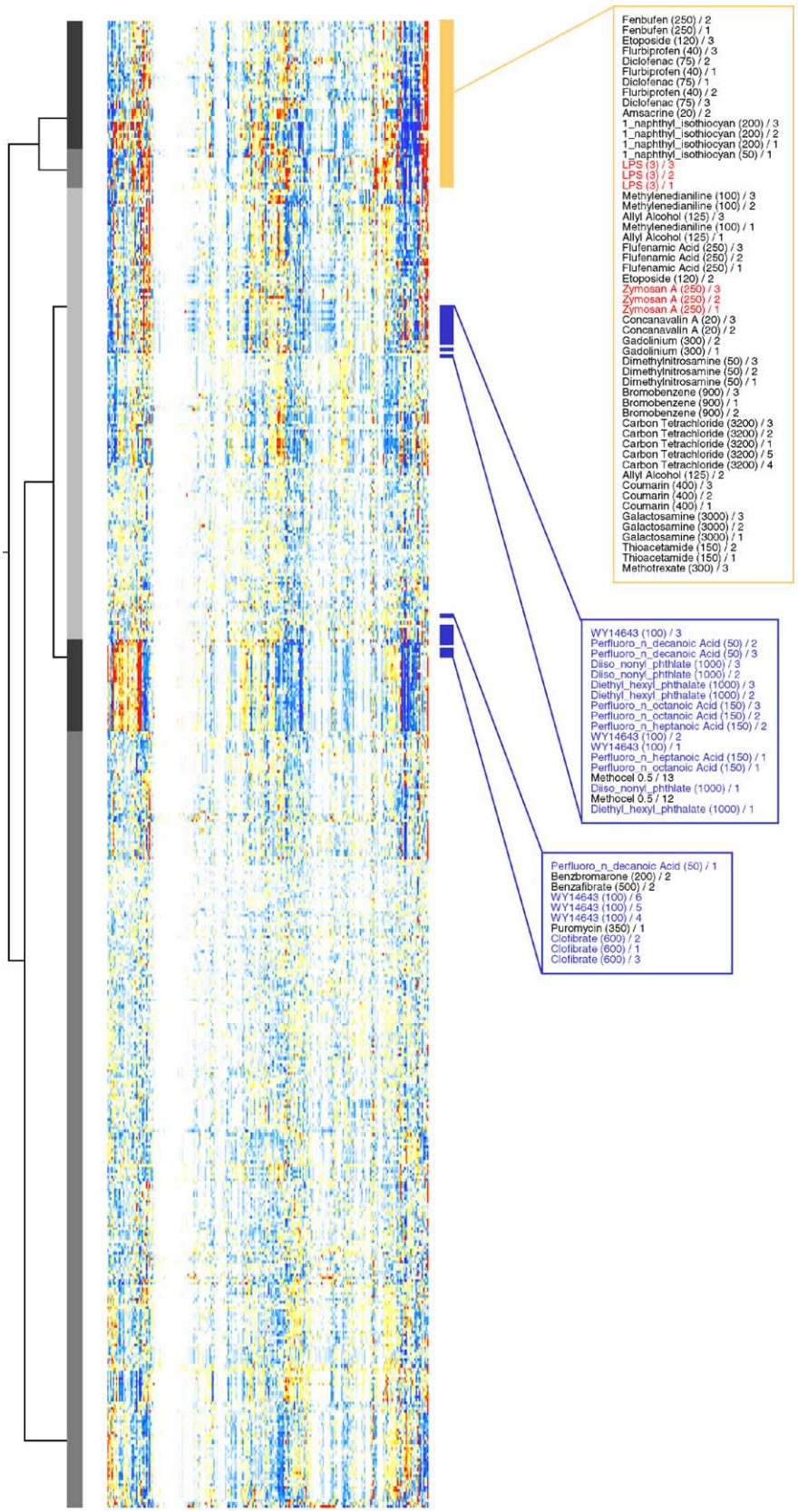

Fig. 1. Clustering of hepatotoxicants (rows) using all 3434 genes (columns) on the Rat MegaA cDNA chip. Red indicates >2.8-fold increases and blue indicates >2.8-fold decreases in gene expression (no change = white) relative to control. The abbreviated dendrogram to the left of the figure shows degree of similarities by clustering, and the expanded list to the right indicates compounds that co-cluster with the training set (red) of LPS (3 mg/kg) and zymosan A (250 mg/kg) using replicate samples from each treatment. Peroxisome proliferators are indicated in blue. The number in parentheses after compound name indicates dose (mg/kg), and the second number is the replicate sample identification number.

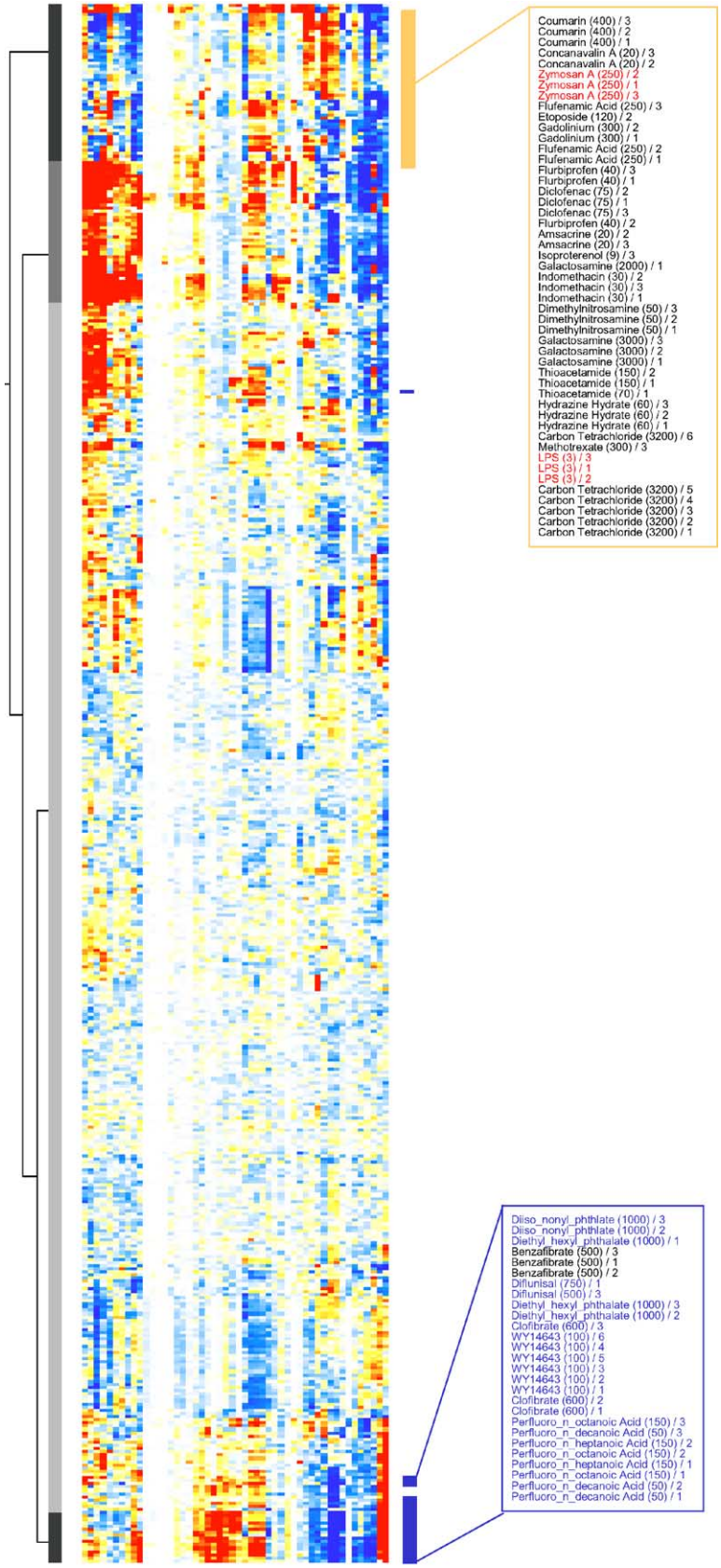

Fig. 2. Clustering of hepatotoxicants using the 50 genes that show the greatest variance across treatments. Terminology is as in Fig. 1, with red indicating >2.8-fold increases and blue indicating >2.8-fold decreases in expression. The expanded list shows replicates from treatments that co-cluster with the training set (red) of LPS and zymosan A.

unsupervised clustering methods above) from all other compounds in our database. This macrophage activator-specific gene expression profile is shown in Table 1 along with the gene ontologies, and the clustering results for this signature gene set is shown in Fig. 3. In addition to the training set of compounds (in red), several other compounds co-clustered with LPS and zymosan A: ANIT and methylenedianiline, the topoisomerase inhibitor amsacrine

Table 1
Genes in macrophage activator signature profiles

Accession	Gene	GO annotation	Comments	Mean[a]
Genes previously reported to change with macrophage activation or the acute phase response				
NM_012747	Signal transducer and activator of transcription 3 (Stat3)	Signal transducer activity; transcription factor activity/Rn_TGF beta signaling pathway	Acute phase response transcriptional factor	0.97
NM_031512	Interleukin 1 beta (IL-1β)	Cytokine activity/Rn_Inflammatory response pathway	Proinflammatory cytokine	0.40
AA819267	Fibrinogen gamma chain-a mrna		Acute phase response protein [11]	0.99
U05675[b]	Fibrinogen B beta chain (Fgb)		Acute phase response protein [11]	0.69
NM_012580	Heme oxygenase (Hmox1)	Heme oxygenase (decyclizing) activity/Rn_Oxidative stress	Acute phase response protein [54,55]	1.54
L31883[c]	Tissue inhibitor of metalloproteinase 1	Rn_Matrix metalloproteinases	Acute phase response protein [56]	1.05
NM_019237	Procollagen C-proteinase enhancer protein (Pcolce)		Collagen processing [57] TIMP-like [58] acute phase response protein?	0.70
NM_017051	Superoxide dismutase 2 (Sod2)	Manganese superoxide dismutase activity/Rn_Oxidative stress	Acute phase response protein [59]	1.43
NM_053318	Hemopexin (Hpx)		Acute phase response protein [60]	0.65
J00696[c]	Orosomucoid 1 (Orm)		Acute phase response protein [11]	2.33
NM_012488	α-2-Macroglobulin (A2m)		Acute phase response protein [11,61]	2.99
L18948[c]	S100 calcium-binding protein A9 (calgranulin B)		Chemotaxis protein; marker for macrophage and neutrophil infiltration [62]	0.96
AF306457[b]	GTPase		Ran GTPase in LPS responses [63]	0.82
NM_017006[b]	Glucose-6-phosphate dehydrogenase (G6pd)	Glucose-6-phosphate 1-dehydrogenase activity/ Rn_Pentose phosphate pathway	[64]; induced by LPS	0.76
AF058791[c]	Maternal G10 transcript (edg2)		Edg lysophospho-lipid signaling system may play a role in inflammation [65]	0.91
NM_024160[c]	Cytochrome b558 α-subunit	Rn_Oxidative stress	Cytokines upregulate cytochrome b558-dependent NAD(P)H oxidase (superoxide; [66])	0.69
AF144756	Fatty acid binding protein 4 (Fabp4)		[67]; LPS induces fatty acid binding proteins	0.96
U13253	Fatty acid binding protein 5, epidermal (Fabp5)		[67]; LPS induces fatty acid binding proteins	1.46
NM_022597	Cathepsin B		Lysosomal protease; [68]; involved in TNFα hepatotoxicity	0.71
X15800	Pyruvate kinase, muscle (Pkm2)	Pyruvate kinase activity/Rn_Glycolysis and gluconeogenesis	[69]; LPS increases pyruvate kinase activity	1.27
NM_012541	Cytochrome P450, 1a2	Monooxygenase activity	LPS represses cytochrome P450 genes [13,70]	−0.97
NM_031543[c]	Cytochrome P450, subfamily 2E, polypeptide 1 (Cyp2e1)	Cytochrome P450 activity; monooxygenase activity	LPS represses cytochrome P450 genes [13,70]	−2.28
NM_031839	Arachidonic acid epoxygenase		LPS represses cytochrome P450 genes [13,70]	−1.14
U40000[c]	Cytochrome P450 monooxygenase		LPS represses cytochrome P450 genes [13,70]	−1.27
NM_012730	Cytochrome P450, subfamily IID2 (Cyp2d2)	Monooxygenase activity	LPS represses cytochrome P450 genes [13,70]	−1.16
M18336	Cytochrome P450, 2c37		LPS represses cytochrome P450 genes [13,70]	−0.66
NM_017158[c]	Cytochrome P450, 2c39		LPS represses cytochrome P450 genes [13,70]	−0.68
NM_012792	Flavin-containing monooxygenase 1 (Fmo1)	Dimethylaniline monooxygenase (*N*-oxide forming) activity	[71]; LPS represses FMO1	−1.52

Table 1 (*Continued*)

Accession	Gene	GO annotation	Comments	Mean[a]
NM_022407[c]	Aldehyde dehydrogenase family 1, member A1 (Aldh1a1)		Aldehyde dehydrogenase activity decreased in inflammation [72]	−1.70
NM_031731	Aldehyde dehydrogenase family 3, subfamily A2 (Aldh3a2)		Aldehyde dehydrogenase activity decreased in inflammation [72]	−1.20
NM_019286	Alcohol dehydrogenase 1 (Adh1)	Alcohol dehydrogenase activity, zinc-dependent		−1.15
NM_017075	Acetyl-coenzyme A acetyltransferase 1 (Acat1)	Acetyl-CoA C-acetyltransferase activity/Rn_Synthesis and degradation of ketone Bodies	[73]; inflammation supresses acetyl CoA acyltransferase	−1.00
NM_012930	Carnitine palmitoyltransferase 2 (Cpt2)	Carnitine *O*-palmitoyltransferase activity/Rn_Fatty Acid degradation; Rn_Mitochondrial fatty acid beta oxidation	[73]; inflammation represses Cpt2	−0.72
NM_013078	Ornithine carbamoyltransferase (Otc)	Ornithine carbamoyltransferase activity	[73]; urea cycle enzyme including Otc mRNAs repressed by LPS and inflammation	−0.83
NM_031589	Glucose-6-phosphatase, transport protein 1 (G6pt1)		[74]; LPS strongly represses glucose-6-phosphatase	−0.98
NM_013098	Glucose-6-phosphatase, catalytic (G6pc)	Rn_Glycolysis and gluconeogenesis	LPS represses glucose-6-phosphatase [74]; peroxisome proliferators induce [75]	−1.90
NM_012588	Insulin-like growth factor binding protein 3	Insulin-like growth factor binding; receptor activity	[30]; IGF-BP3 is repressed by LPS	−0.77
NM_053329[b]	Insulin-like growth factor binding protein, acid labile subunit (Igfals)			−1.30
NM_022245[c]	Cytochrome b5		[76]; LPS decreased cytochrome b5 in rat liver	−1.14
NM_012504	ATPase, Na^+K^+ transporting, alpha 1	Sodium/potassium-exchanging ATPase activity	[77]; Na^+K^+ ATPase activity selectively decreased by LPS	−0.71
NM_012657	Serine protease inhibitor (Spin2b)		[78]; LPS represses growth hormone-induced spin2	−0.95
NM_024132[b]	Fatty acid amide hydrolase (Faah)	Amidase activity	LPS inhibits Faah; [79]	−0.57
AA858962[b]	cDNA clone similar to retinol-binding protein (RBP)		[31]; LPS, inflammation decrease RBPs	−0.59
Genes reported to change in response to peroxisome proliferators				
AA817964	Similar to MMU32684 mouse serum paraoxonase (PON)		sp: P55159, PON1_RAT serum paraoxonase/arylesterase 1 (PON1); decreased by peroxisome proliferators [80]	−0.64
AA859342	cDNA clone similar to 17β-hydroxysteroid dehydrogenase type 2		17β-Hydroxysteroid dehydrogenase-like enzyme in rat is induced by peroxisome proliferators [81]	−0.91
AW915938[c]	EST		pdb: 22G*S*-glutathione *S*-transferase P1-1 Y49f-like (69%); [82], glutathione *S*-transferases inhibited by peroxisome proliferators	−1.42
AA892234	EST		ref: NP_079845.1, microsomal glutathione *S*-transferase 3 [82], glutathione *S*-transferases inhibited by peroxisome proliferators	−1.66
BE109053[c]	EST		pir: I60307, I60307 β-galactosidase-like (*E. coli* 87%/54 aa) [83], peroxisome proliferators repress hepatic β-galactosidases	0.67
D00569	2,4-Dienoyl CoA reductase 1, mitochondrial (Decr1)	Rn_Fatty Acid synthesis; Rn_Mitochondrial fatty acid beta oxidation	2,4-Dienoyl-CoA reductase is induced by the peroxisome proliferatorn clofibrate [84]	−1.15
D90109	Fatty acid coenzyme A ligase, long chain 2 (Facl2)	Acetate-CoA ligase activity/ Rn_Fatty Acid degradation; Rn_Mitochondrial fatty acid beta oxidation	Expression decreased in PPARα knockout mice [85]	−1.55
NM_031565	Carboxylesterase 1		Carboxylesterases are induced by peroxisome proliferators [86,87]	−2.11

Table 1 (*Continued*)

Accession	Gene	GO annotation	Comments	Mean[a]
M20629	Esterase 2 (Es2)	Serine esterase activity	Carboxylesterases are induced by peroxisome proliferators [86,87]	−1.35
M33648	3-Hydroxy-3-methylglutaryl-coenzyme A synthase 2 (Hmgcs2)	Hydroxymethylglutaryl-CoA synthase activity/Rn_Cholesterol biosynthesis; Rn_Synthesis and degradation of ketone bodies	Ketogenic enzyme induced by PPARα [88]	−1.20
NM_016999	Cytochrome P450, subfamily 4B, polypeptide 1 (Cyp4b1)	Monooxygenase activity	Peroxisome proliferators induce CYP4b1 (= CYP4A1)	−1.38
NM_017306	Dodecenoyl-coenzyme A delta isomerase (Dci)	Dodecenoyl-CoA delta-isomerase activity/Rn_Mitochondrial fatty acid beta oxidation	3,2-*trans*-Enoyl-CoA isomerase is induced by peroxisome proliferators [84]	−1.42
NM_022594[c]	Enoyl coenzyme A hydratase 1 (Ech1)		Enoyl coenzyme A hydratase is induced by peroxisome proliferators [89]	−1.64
NM_022936	Cytosolic epoxide hydrolase		Cytosolic epoxide hydrolase is induced by peroxisome proliferators [90]	−1.84
NM_031736[c]	Solute carrier family 27 (fatty acid transporter), member 32 (Slc27a2)		Fatty acid transporters are induced by peroxisome proliferators [91]	−1.01
AI105167	EST		Selenium binding protein 2 [92] reduced by peroxisome proliferators	−1.24
NM_031587	Peroxisomal membrane protein 2 (Pxmp2)			−0.70
NM_016986	Acetyl-coenzyme A dehydrogenase, medium chain	Acyl-CoA dehydrogenase activity/Rn_Fatty Acid degradation; Rn_Mitochondrial fatty acid beta oxidation	[93]; induced by PPARα (Acadm)	−1.08
M89902	3-Hydroxybutyrate dehydrogenase (heart, mitochondrial)	Rn_Synthesis and degradation of ketone bodies	[94]; activity inhibited by peroxisome proliferators	−1.38
J05132	UDP glycosyltransferase 1 family, polypeptide A6	Rn_Androgen and estrogen metabolism	[95]; peroxisome proliferators induce certain UDP-glucuronosyltransferases	−0.78
NM_017340[b]	Acyl-CoA oxidase (RATACOA1)		[93]; induced by peroxisome proliferators	−1.32
NM_017332[b]	Fatty acid synthase (RATFASA)	Rn_Fatty Acid synthesis	[96]; FAS induced after removal of a peroxisome proliferator	0.70
ER stress, chaperone protein and heat shock protein genes				
BE109544	EST		ref: NP_064363.1, heat shock protein 030 (Mus musculus) 96%/91 aa	0.66
NM_032614	Thioredoxin-like 2 (Txnl2)		Multifunctional ER chaperone and stress response protein	0.93
NM_013067	Ribophorin I (Rpn1)		Oligosaccharyltransferase and marker of rough ER; linked to DAD1, the defender against apoptotic cell death [97] upregulated in activated lymphocytes [98]	0.82
NM_012998	Protein disulfide isomerase (prolyl 4-hydroxylase, β-polypeptide) (P4hb)	Procollagen-proline, 2-oxoglutarate-4-dioxygenase activity; protein disulfide isomerase activity	Multifunctional ER chaperone and stress response protein; collagen processing [99]	1.10
NM_053961[c]	Endoplasmic reticulum protein 29		Multifunctional ER chaperone and stress response protein	0.87
NM_022399[c]	Calreticulin		Multifunctional ER chaperone and stress response protein [100]	1.19
NM_031580	Glucose regulated protein, 58 kDa (Grp58)		Multifunctional ER chaperone and stress response protein [45]	0.96
NM_022536	Cyclophilin B		Multifunctional ER chaperone and stress response protein; collagen processing [99]	0.82
NM_019905	Calpactin I heavy chain		ER membrane trafficking protein	1.24
NM_017199[c]	Signal sequence receptor 4 (Ssr4)		ER membrane trafficking protein	0.66
NM_022278[b]	Glutaredoxin (Glrx)		Multifunctional oxstress protein	−0.62

Table 1 (*Continued*)

Accession	Gene	GO annotation	Comments	Mean[a]
Cytoskeletal protein genes				
NM_006082[c]	Tubulin, alpha, ubiquitous	Structural molecule activity	Cytoskeletal protein	0.59
NM_017147	Cofilin 1 (Cfl1)	Rn_G13 signaling pathway	Cytoskeletal regulator	0.93
NM_022298	α-Tubulin		Cytoskeletal protein	1.44
U66461[c]	Dynein, cytoplasmic, light chain 1		Cytoskeletal and organelle motility	0.77
NM_021261	Thymosin, beta 10 (Tmsb10)		Cytoskeletal regulator; immune cell mitogen (?) [101]	0.66
NM_031144	Actin, beta		Cytosketal protein	0.96
NM_017343[b]	Myosin regulatory light chain (MRLCB)		Cytoskeletal	0.77
NM_031140[b]	Vimentin (Vim)			0.96
Metabolism genes				
NM_030850	Betaine-homocysteine methyltransferase	Rn_Methionine metabolism		−2.05
NM_017201	*S*-Adenosylhomocysteine hydrolase (Ahcy)	Rn_Methionine metabolism		−1.28
NM_012695	Rat senescence marker protein 2A gene, exons 1 and 2 (Smp2a)	Sulfotransferase activity		−0.88
NM_031834	Sulfotransferase family 1A, phenol-preferring, member 1 (Sult1a1)			−1.22
NM_022402	Acidic ribosomal protein P0	Rn_Ribosomal proteins		0.52
NM_021593	Kynurenine 3-hydroxylase			−0.59
NM_031834[b]	Minoxidil sulfotransferase (PST-1)			−1.36
U18762[b]	Liver microsomal retinol dehydrogenase type I			−0.60
NM_022251[b]	Aminopeptidase A (Enpep)			−0.70
NM_024127[b]	DNA-damage-inducible transcript 1 (Gadd45a)			0.59
Other functions and ESTs				
BI285007	EST		ref: NP_036558.1, splicing factor 3b, subunit 3, 130 kDa; spliceosome-associated protein 130	−1.85
AA818627	cDNA clone similar to insulin-induced growth response protein CL-6		ref: NP_005533.1, insulin-induced gene 1; insulin-induced gene 1 78.46%/195 aa	−1.63
BI282332	EST		ref: NP_077128.2, ethanol-induced 6 (Mus musculus) (53%)	−1.05
BI281813	EST		sp: P38718, P044_RAT 0-44 protein (100%)	−0.89
AA900340	EST			−0.93
AA818998	EST			−0.92
AI169152	EST			−0.61
AA849738[c]	EST			1.03
BE098355[c]	EST			1.33
BI291463	EST		ref: NP_079785.1, RIKEN cDNA 2310008M10 (Mus musculus) 100.00%/149 aa	0.94
AA858899	EST			1.34
BI285489[c]	EST		ref: NP_076116.1, myo-inositol 1-phosphate synthase A1; yeast ER stress, Stroobants, 1999	1.41
BI303631	EST		ref: NP_113600.1, GABA(A) receptor-associated protein like 1; early estrogen-regulated protein; intracellular membrane trafficking	−0.87
NM_022282	Discs, large (Drosophila) homolog 2 (chapsyn-110)		Membrane associated guanylate kinase-related protein	0.79
NM_013132	Annexin 5 (Anxa5)	Anticoagulant activity; calcium ion binding; calcium-dependent phospholipid binding		0.94
D17310	3α-Hydroxysteroid dehydrogenase	Rn_C-21 steroid hormone metabolism; Rn_Glucocorticoid and mineralocorticoid metabolism		−1.02
D88666	Phosphatidylserine-specific phospholipase A1			0.86

Table 1 (*Continued*)

Accession	Gene	GO annotation	Comments	Mean[a]
AA892916[b]	EST			−0.78
AI406939[b]	EST			−0.74
BF555189[b]	EST			−0.66
NM_017126[b]	Ferredoxin 1 (Fdx1)			−0.87
NM_022505[b]	Rhesus blood group (Rh)			−0.74
M27905[b]	Ribosomal protein L21	Rn_Ribosomal proteins		0.63
L01123[b]	Ribosomal protein S13 (RPS13)			0.76

[a] Mean of $\log_2$(ratio) of all samples treated with microphage activators.
[b] Genes in the predictive gene list only.
[c] Genes in both macrophage activator gene lists.

(20 mpg), *trans*-anethole (600 mpg), and a number of NSAIDs: fenbufen, indomethacin and ibuprofen (500 mpg).

Most of these 100 macrophage activator-specific genes fell into three coordinately regulated groups of genes—acute phase proteins, endoplasmic reticulum stress/chaperone proteins, and peroxisome proliferator-responsive genes (Table 1). While this macrophage activator-specific gene expression profile gave insights into mechanisms of action, many of the genes were redundant, and it was useful to have a minimal non-redundant gene set that separated macrophage activators from other compounds. A multivariate gene selection approach was applied, using Partek™ software, to select a minimal gene set that best separates LPS, zymosan A and co-clustered putative macrophage activators from all other remaining samples. Forty-three genes selected by forward selection (Table 1) could almost perfectly separate members of the macrophage activator training set from all other compounds (Fig. 4). Among the macrophage activator training set, diclofenac, flurbiprofen, and some replicates of carbon tetrachloride and etoposide failed to co-cluster, and only one methylenedianiline replicate outside of the training set co-clustered with LPS and zymosan A (Fig. 4).

3.3. Independent confirmation of macrophage activation by cytokine RNA levels

Macrophage activation is usually defined by proinflammatory cytokine production (particularly TNFα, IL-1β and IL-6) along with inducible nitric oxide and/or superoxide production. Cytokines and free radicals are known to regulate many genes in the liver and are necessary for macrophage-induced hepatotoxicity. Although some cytokine genes were present on our microarray, the low abundances of cytokine mRNAs in the small fraction of Kupffer cells in liver samples were generally below our limit of detection by microarray. Even by PCR, basal levels of cytokine and iNOS mRNA were not detectable in all experiments. PCR did show pronounced increases in TNFα, IL-1β, IL-6 and iNOS mRNAs for compounds identified as macrophage activators by microarray analyses (Table 2). LPS, zymosan A, allyl alcohol, coumarin, dimethylnitrosamine, or thioacetamide administration produced large increases in all four mRNAs. At least three of these four mRNA markers of macrophage activation increased with galactosamine, diclofenac, etoposide, flufenamic acid, and ANIT treatments. Carbon tetrachloride, concanavalin A, and gadolinium chloride failed to increase more than one of the four mRNAs although there is substantial literature linking these three compounds to macrophage activation. The excellent agreement between PCR and microarray analysis confirmed the value of the above genes sets in identifying LPS and zymosan A-like compounds.

3.4. Inverse gene regulation by macrophage activators and peroxisome proliferators

Interestingly, a large number of peroxisome proliferator-induced genes were selected for the macrophage activator gene signature profiles, and most of these genes were repressed by macrophage activators (Table 1). A peroxisome proliferator-specific gene expression profile composed of 100 clones was constructed as described for macrophage activators using transcriptional responses to clofibrate, WY 14643, diethylhexylphthalate, diisononylphthalate, perfluorodecanoic acid, perfluoroheptanoic acid, and perfluorooctanoic acid as training set samples (Table 3). Using this large training set of peroxisome proliferators, the gene set cleanly separated the peroxisome proliferators from all other samples (Fig. 5; one stray replicate of diethylnonyl phthlate may represent a failed sample). A second cluster distinct from the training set, but closer to peroxisome proliferators than to all other compounds, contained many compounds (benzfibrate, benzbromarone, dichloroacetate, valproic acid and the NSAIDs diflunisal, fenbufen and ibuprofen) known to have PPARα agonist activity at high dose. Some of these compounds, notably benzfibrate and valproic acid, also have PPARβ/δ agonist activity, which might have contributed to their separation from the training set cluster. As expected, macrophage activators clustered separately from peroxisome proliferators and other compounds using this peroxisome proliferator gene set (Fig. 5). Among the 11 genes common to both the macrophage activator and the peroxisome proliferator gene expression profiles (Tables 1 and 3), eight were oppositely regulated in the two classes of hepatotoxicants.

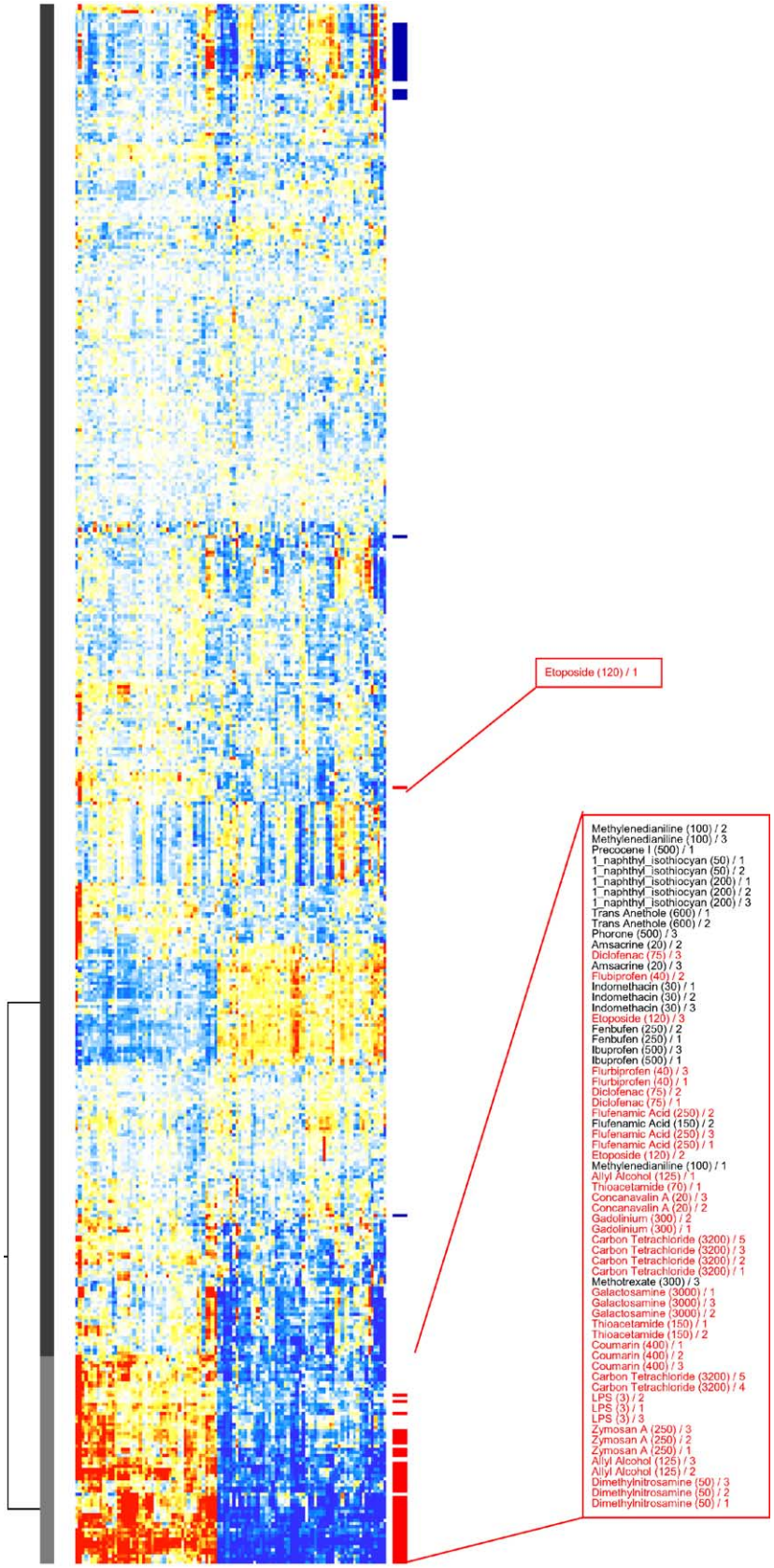

Fig. 3. A macrophage activator gene signature pattern. Compounds that co-cluster with LPS and zymosan A in both Figs. 1 and 2 were chosen as macrophage activation training set samples (red) and the 100 clones (genes listed in Table 1) that statistically best separate this training set from all other samples were used for clustering. Terminology is as in Fig. 1. Red indicates >2.8-fold increases and blue indicates >2.8-fold decreases in expression.

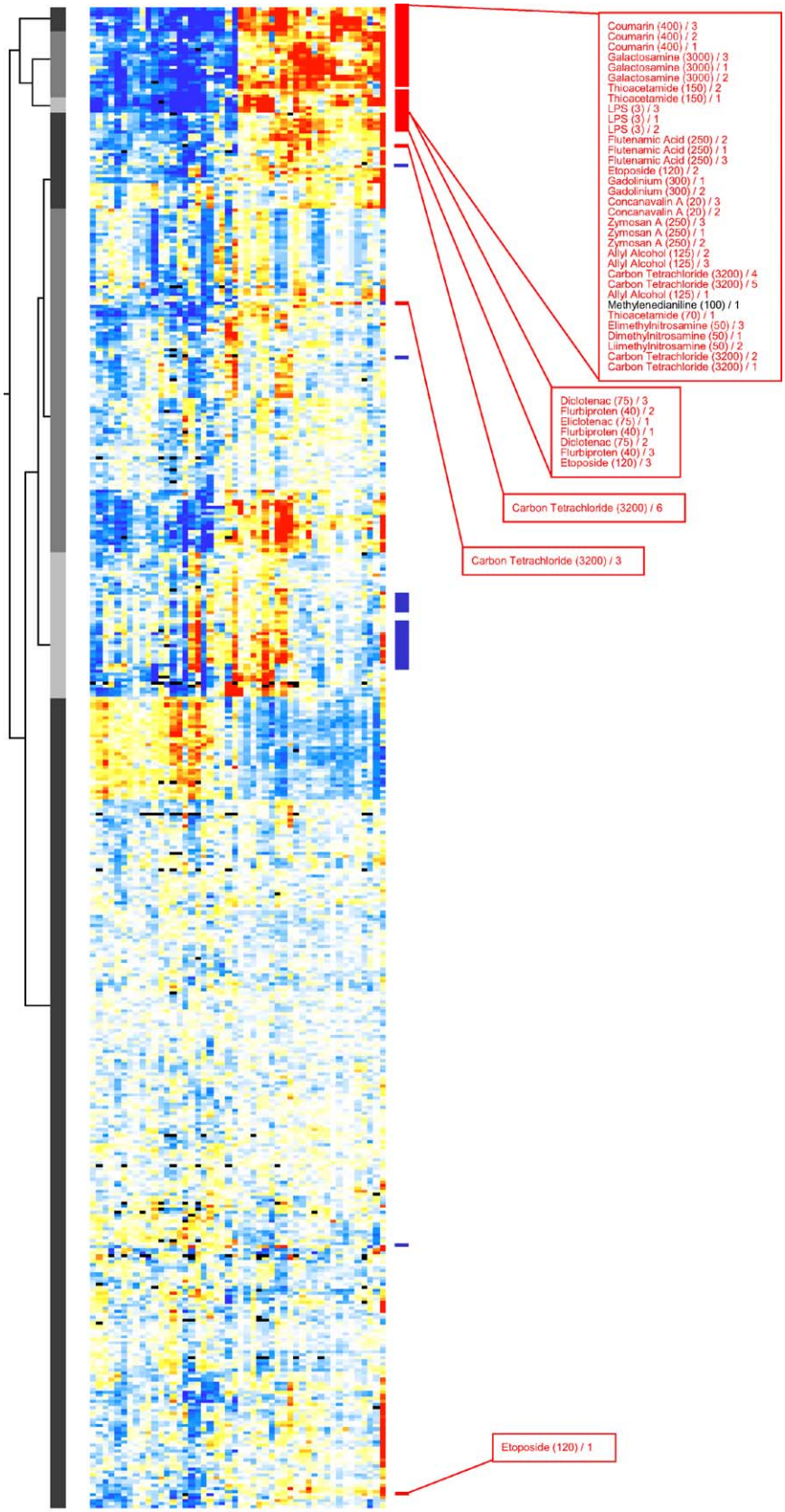

Fig. 4. A macrophage activator gene signature pattern derived from multivariate analysis. Using the same training set samples (in red) as in Fig. 3, 43 non-redundant genes (listed in Table 1) were selected by a multivariate procedure (see Section 2 for details). Clustering with these genes best separated the training set from all other compounds. Terminology is as in Fig. 1. Red indicates >2.8-fold increases and blue indicates >2.8-fold decreases in expression.

Table 2
Hepatic cytokine RNA changes relative to control (=1.0) measured by TaqMan PCR

Treatment	TNFα		IL-1β		IL-6		iNOS	
	Average	S.E.M.	Average	S.E.M.	Average	S.E.M.	Average	S.E.M.
ANIT 200 mg/kg	**4.9**	**1.7**	**1.7**	**0.3**	**41.2**	**6.8**	**56.3**	**40**
Allyl alcohol 125 mg/kg	**13.2**	**5.6**	**6.8**	**3.5**	**111.3**	**32.9**	**4482**	**2857.1**
Aspirin 600 mg/kg	0.5	0.1	0.3	0.1	0.6	0	1	0
Busulfan 100 mg/kg	1.1	0.5	0.4	0.2	1	0	1	0
Cadmium 75 mg/kg	0.9	0.1	0.4	0.1	1	0	1	0
Carmustine 30 mg/kg	2.8	0.6	0.6	0.2	1.1	0.3	1	0
Carbon tetrachloride 3200 mg/kg	1.6	0.5	1.4	0.7	1	0	**669.1**	**408.5**
Chlorambucil 25 mg/kg	1.8	0.4	0.4	0.2	1	0	1	0
Concanavalin A 20 mg/kg	0.9	0.3	0.6	0.3	**4.5**	**1.6**	1	0
Coumarin 400 mg/kg	**62.1**	**17.9**	**15.4**	**1.1**	**599.5**	**171.6**	**30260.4**	**7014.8**
Diclofenac 75 mg/kg	**4.7**	**1.7**	**1.6**	**0.3**	4.9	4	**12.2**	**6.1**
Dieldrin 45 mg/kg	**2.2**	**0.1**	**1.4**	**0.2**	1.3	0.2	1	0
Diethylhexylpthalate 1000 mg/kg	0.2	0	0.1	0	0.5	0	1	0
Diflunisal 500 mg/kg	1.4	0.7	**2.6**	**0.9**	1	0	1	0
Diflunisal 750 mg/kg	**5.3**	**2.4**	0.1	0.1	0.8	0.3	2.2	1.2
Dimethylnitrosamine oral 50 mg/kg	**50.8**	**11.4**	**7.4**	**1.6**	**508.9**	**34.4**	**3720.3**	**1731.4**
Erythromycin estolate 1500 mg/kg	0.3	0	0.3	0.1	0.7	0.1	1	0
Ethinyl estradiol 500 mg/kg	1.1	0.2	0.9	0.6	0.6	0.1	1	0
Etoposide 120 mg/kg	**6.2**	**0.9**	0.8	0.4	**3.4**	**0.4**	**51.3**	**28.9**
Flufenamic acid 150 mg/kg	1.6	0.5	1.4	0.4	1.3	0.1	26.8	14.4
Flufenamic acid 250 mg/kg	**4.2**	**1.6**	1.4	0.4	**2.3**	**0.9**	**84.1**	**61.8**
Fluoxetine 100 mg/kg	7.2	1.8	1.5	0.4	1.1	0.1	1	0
Gadolinium chloride 300 mg/kg	1	0.1	0.2	0.1	1.6	1	**10.1**	**8.9**
Galactosamine 3000 mg/kg	**20.5**	**4.6**	**4.1**	**0.4**	**7.5**	**1.7**	1	0
Gentamycin 750 mg/kg	10.8	4.1	4.7	2	1.7	0.7	157.1	156.1
Hexachlorocyclohexane glindane 80 mg/kg	**3.8**	**0.1**	1.3	0.6	1	0	1	0
LPS 3 mg/kg	**5.5**	**1.6**	**22.7**	**5.7**	**10.6**	**2**	**432.7**	**139.3**
Nimesulide 500 mg/kg	**8.8**	**2.9**	1.5	0.6	1.2	0.2	**12.6**	**6.4**
Paraquat 100 mg/kg	**10.3**	**1.3**	**2.3**	**0.2**	1	0	1	0
Perfluoro-*n*-heptanoic acid 150 mg/kg	1.1	0.6	1.6	1.4	1.8	0.7	1	0
Phenacetin 1200 mg/kg	3.5	2.3	1.4	0.6	1	0	3.6	2.6
Pulegone 400 mg/kg	**3**	**0.2**	1.2	0.2	1	0	1	0
Rifampin 600 mg/kg	0.6	0.2	0.6	0.2	0.6	0	1	0
Rotenone 100 mg/kg	0.5	0.4	0.7	0.4	1.6	0.6	1	0
Rotenone 6 mg/kg	**2.1**	**0.1**	0.8	0.1	1	0	1.1	0.1
Thioacetamide 150 mg/kg	**74.9**	**8.8**	**19.3**	**5.7**	**41.6**	**5.2**	**4311.9**	**1386.2**
Troglitazone 500 mg/kg	2.3	1	**2.6**	**0.7**	1	0	1	0
Valproic acid 1000 mg/kg	0.9	0.5	0.8	0.1	1	0	1	0
Vitamin A 200 mg/kg	**5.3**	**0.2**	1	0.5	1.2	0.2	1	0
Vitamin A 100 mg/kg	1.3	0.1	1.1	0.3	0.7	0.2	1	0
WY 14643 100 mg/kg	1.3	0.4	0.6	0.1	0.6	0.1	1	0
Zymosan A 250 mg/kg	**10.6**	**2.4**	**4.1**	**1.2**	**92.9**	**20.7**	**501.9**	**253.1**

Bolded numbers show significant increase in mRNA relative to control based on analysis by TaqMan PCR. RNA was from the same samples used for microarray analysis. For IL-6 and iNOS, control levels were usually undetectable at 40 and 60 cycles, but 40 cycles was taken as the control threshold. The changes in these RNAs are thus underestimates. If IL-6 or iNOS RNA was detectable at 39 cycles in two or more of three animals from a treatment, the effect was deemed significant.

4. Discussion

In the present study hepatic gene expression patterns elicited by the macrophage activators LPS and zymosan A were compared with responses to approximately 100 prototypical compounds, mostly hepatotoxicants, after 24 h of treatment. Using unbiased, unsupervised clustering methods, several compounds consistently co-clustered with LPS and zymosan A. Most of these hepatotoxicants are known to activate macrophages in rat liver: allyl alcohol [18], carbon tetrachloride [19], dimethylnitrosamine [20], galactosamine [21], gadolinium chloride [22,23], thioacetamide [24], concanavalin A [25] and a number of NSAIDs have all been previously associated with macrophage activation and/or gut-derived endotoxin entry [26–28]. Additionally our data showed that coumarin, and etoposide closely resembled LPS and zymosan A in their hepatic transcriptional profiles. TNFα, IL-1β, IL-6 and iNOS mRNA measurements using TaqMan PCR confirmed activation of macrophages by these compounds. Using these co-clustered compounds as a training set, signature gene profiles for macrophage activators were determined. In addition to the expected effects on acute phase and immune activation genes and effects to repress xenobiotic metabolic

Table 3
Genes in peroxisome proliferator signature profile

Accession	Gene	GO annotation	PP agonists	LPS like
Genes previously reported to change with macrophage activation or the acute phase response				
NM_031589[a]	Glucose-6-phosphatase, transport protein 1 (G6pt1)		−1.11	−0.98
AA858661	Similar to mouse major histocompatibility locus class III region: butyrophilin-like protein gene		−0.47	−0.31
NM_012656	Secreted acidic cystein-rich glycoprotein (osteonectin) (Sparc)		−0.75	−0.30
NM_017055	Transferrin (Tf)	Iron ion transporter activity	−0.85	−0.27
AA858930	Similar to human 3′,5′-cyclic AMP phosphodiesterase		−0.46	−0.22
NM_017020	Interleukin 6 receptor (IL-6R)	Interleukin receptor activity	−0.48	−0.21
NM_012656	Secreted acidic cystein-rich glycoprotein (osteonectin) (Sparc)		−0.68	−0.21
NM_017080	Hydroxysteroid 11-β-dehydrogenase 1 (Hsd11b1)	11β-Hydroxysteroid dehydrogenase activity/ Rn_C-21 steroid hormone metabolism; Rn_Glucocorticoid and mineralocorticoid metabolism	−0.70	−0.14
Y07744	UDP-*N*-acetylglucosamine-2-epimerase/ *N*-acetylmannosamine kinase (Uae1)		−0.86	−0.11
NM_019135	Tumor necrosis factor superfamily, member 8 (Tnfrsf8)		−0.24	−0.02
NM_021587	LanC (bacterial lantibiotic synthetase component C)-like 1 (Ltbp1)		−0.25	0.08
M83143	Sialyltransferase 1 (β-galactoside α-2,6-sialytransferase) (Siat1)	β-Galactosamide α-2,6-sialyltransferase activity	−0.57	0.23
NM_019132	Guanine nucleotide-binding protein G-s, α-subunit		−0.54	0.36
NM_012811	Milk fat globule-EGF factor 8 protein (Mfge8)	Cell adhesion molecule activity	−0.73	0.44
NM_016995	Complement component 4 binding protein, beta (C4bpb)		−0.66	0.49
M11794	Metallothionein (Mt1a)	Rn_Oxidative stress	−2.15	0.53
NM_017258	B-cell translocation gene 1		−0.51	0.63
U76206	G protein-coupled receptor 105 (Gpr105)		0.33	0.01
NM_022928	G protein-coupled receptor kinase 2, groucho gene-related (Drosophila) (Gprk2l)	G protein-coupled receptor activity	0.33	−0.48
Genes reported to change in response to peroxisome proliferators				
X64589	Cyclin B1 (Ccnb1)	Rn_Cell cycle	0.30	0.02
J03752	Microsomal glutathione *S*-transferase 1 (Mgst1)	Rn_Oxidative stress	0.32	0.14
NM_012930[a]	Carnitine palmitoyltransferase 2 (Cpt2)	Carnitine *O*-palmitoyltransferase activity/ Rn_Fatty Acid degradation; Rn_Mitochondrial fatty acid beta oxidation	0.65	−0.72
M30596	Malic enzyme 1 (Me1)	Malic enzyme activity	0.73	−0.02
NM_022594[a]	Enoyl coenzyme A hydratase 1 (Ech1)		0.77	−1.64
NM_031853	Diazepam binding inhibitor (Dbi)	Lipid binding	0.77	0.08
NM_017075[a]	Acetyl-coenzyme A acetyltransferase 1 (Acat1)	Acetyl-CoA C-acetyltransferase activity/ Rn_Synthesis and degradation of ketone bodies	0.78	−1.00
NM_017306[a]	Dodecenoyl-coenzyme A delta isomerase (Dci)	Dodecenoyl-CoA delta-isomerase activity/ Rn_Mitochondrial fatty acid beta oxidation	0.79	−1.42
AB010632	Carboxylesterase 2 (intestine, liver)		0.87	−0.38
M33936	Cytochrome P450 4A3		0.90	−0.67
NM_013214	Brain acyl-CoA hydrolase		1.00	−0.29
NM_031703	Aquaporin 3 (Aqp3)		1.04	−0.06
NM_017340[a]	Acyl-CoA oxidase		1.28	−1.32
NM_016999[a]	Cytochrome P450, subfamily IVB, polypeptide 1 (Cyp4b1)		1.49	−1.38
NM_031561	cd36 antigen	Fatty acid binding; receptor activity	1.52	0.02
NM_031315	Cytosolic acyl-CoA thioesterase 1 (Cte1)		3.35	−0.77
ER stress, chaperone protein and heat shock protein genes				
NM_012998[a]	Protein disulfide isomerase (prolyl 4-hydroxylase, β-polypeptide) (P4hb)	Procollagen-proline, 2-oxoglutarate-4-dioxygenase activity; protein disulfide isomerase activity	−0.68	1.10
NM_022399[a]	Calreticulin		−0.63	1.19
NM_031970	Heat shock 27 kDa protein 1 (Hspb1)		0.58	0.11
NM_012670	T-complex 1 (Tcp1)	ATP binding; chaperone activity	0.33	−0.17
NM_031580[a]	Glucose regulated protein, 58 kDa (Grp58)		−0.48	0.96

Table 3 (*Continued*)

Accession	Gene	GO annotation	PP agonists	LPS like
Cytoskeletal protein genes				
NM_017083	Myosin 5B		0.46	−0.04
NM_006082[a]	Tubulin, alpha, ubiquitous	Structural molecule activity	0.81	0.59
AF306457	RAN, member RAS oncogene family		0.96	0.82
X91651	*R. norvegicus* NTF2 gene		0.47	0.26
NM_019143	Fibronectin 1 (Fn1)	Rn_Inflammatory response pathway	0.31	0.04
Other functions and ESTs				
BE110688	EST		−2.26	0.20
BI296033	EST		0.24	−0.06
BE109139	EST		0.30	0.05
BI288833	EST		0.30	−0.04
BG378729	EST		0.37	−0.20
BI278268	EST		0.42	−0.85
BE112899	EST		0.44	−0.25
BG380656	EST		0.44	−0.28
BI294947	EST		0.46	0.12
BF281192	EST		0.46	0.07
AW915993	EST		0.52	−0.02
BG666786	EST		0.63	0.09
BI296125	EST		0.65	0.04
BG663099	EST		0.36	0.09
NM_031531	Serine protease inhibitor (Spin2c)		−0.88	0.51
NM_022526	rap7a		−0.76	0.48
M84000	Pregnancy-zone protein		−0.61	0.20
NM_012898	2α-HS-glycoprotein (Ahsg)	Cysteine protease inhibitor activity	−0.60	−0.16
NM_012741	K-kininogen, differential splicing leads to HMW Kngk (Kng_v1)	Cysteine protease inhibitor activity	−0.55	0.21
M96674	Glucagon receptor (Gcgr)	Rn_GPCRs, class b secretin-like	−0.54	−0.57
NM_022960	Aquaporin 9 (Aqp9)		−0.43	0.21
NM_012521	Calbindin 3 (Calb3)	Calcium ion binding	−0.26	0.13
AF000578	Cell division cycle 5-like (*S. pombe*) (Cdc5l)		−0.35	−0.07
X81193	Cysteine-rich protein 3 (Csrp3)		−0.28	−0.02
NM_012581	Homeo box A2 (Hoxa2)	Transcription factor activity	−0.24	−0.05
NM_031553	Nuclear transcription factor, Y beta (Nfyb)	Transcription factor activity	−0.38	−0.05
M38759	Androgen binding protein (ABP)		1.00	0.17
NM_022514	Ribosomal protein L27		0.81	0.65
NM_019373	Apolipoprotein M		0.77	−0.17
NM_012716	Solute carrier family 16, member 1 (Slc16a1)	Carrier activity; monocarboxylic acid transporter activity	0.72	0.13
NM_033236	Proteasome (prosome, macropain) 26*S* subunit, ATPase (Psmc2)	Rn_Proteasome degradation	0.71	0.17
NM_017177	Choline/ethanolamine kinase (Chetk)		0.70	−0.22
AF157026	Type IIb sodium–phosphate transporter		0.67	0.08
NM_017321	Iron-responsive element-binding protein	RNA binding; aconitate hydratase activity	0.60	−0.55
NM_024135	LIM motif-containing protein kinase 2 (Limk2)	ATP binding; protein kinase activity	0.37	0.12
NM_001402	Human eukaryotic translation elongation factor 1 alpha 1 (EEF1A1)		0.28	−0.18
NM_012695	Senescence marker protein 2A gene (Smp2a)	Sulfotransferase activity	−0.82	−0.88
NM_019249	Protein tyrosine phosphatase, receptor type, F (Ptprf)		−0.71	−0.35
NM_032080	Glycogen synthase kinase 3 beta (Gsk3b)	Rn_Cell cycle; Rn_Glycogen metabolism; Rn_Wnt Signaling	−0.52	−0.42
NM_019370	Alkaline phosphodiesterase		−0.45	−0.41
M31322	Sperm membrane protein (YWK-II)		−0.48	−0.39
NM_017170	Serum amyloid P-component (Sap)		−0.53	−0.35

Mean of $\log_2$(ratio) of all samples treated with peroxisome proliferators or microphage activators.

[a] Also in microphage activator gene list.

pathways, (particularly the extensively studied cytochrome P450 genes) there were some unexpected pathways in our signature gene profile for macrophage activators. Strong inductions of ER stress/chaperone protein genes were noted and specific hepatic gene regulation by macrophage activators was also observed to be largely inverse to that by peroxisome proliferators.

There were abundant macrophage activation-responsive genes in the liver, and our derived signature genes were a subset of the "best" (most responsive, most significantly

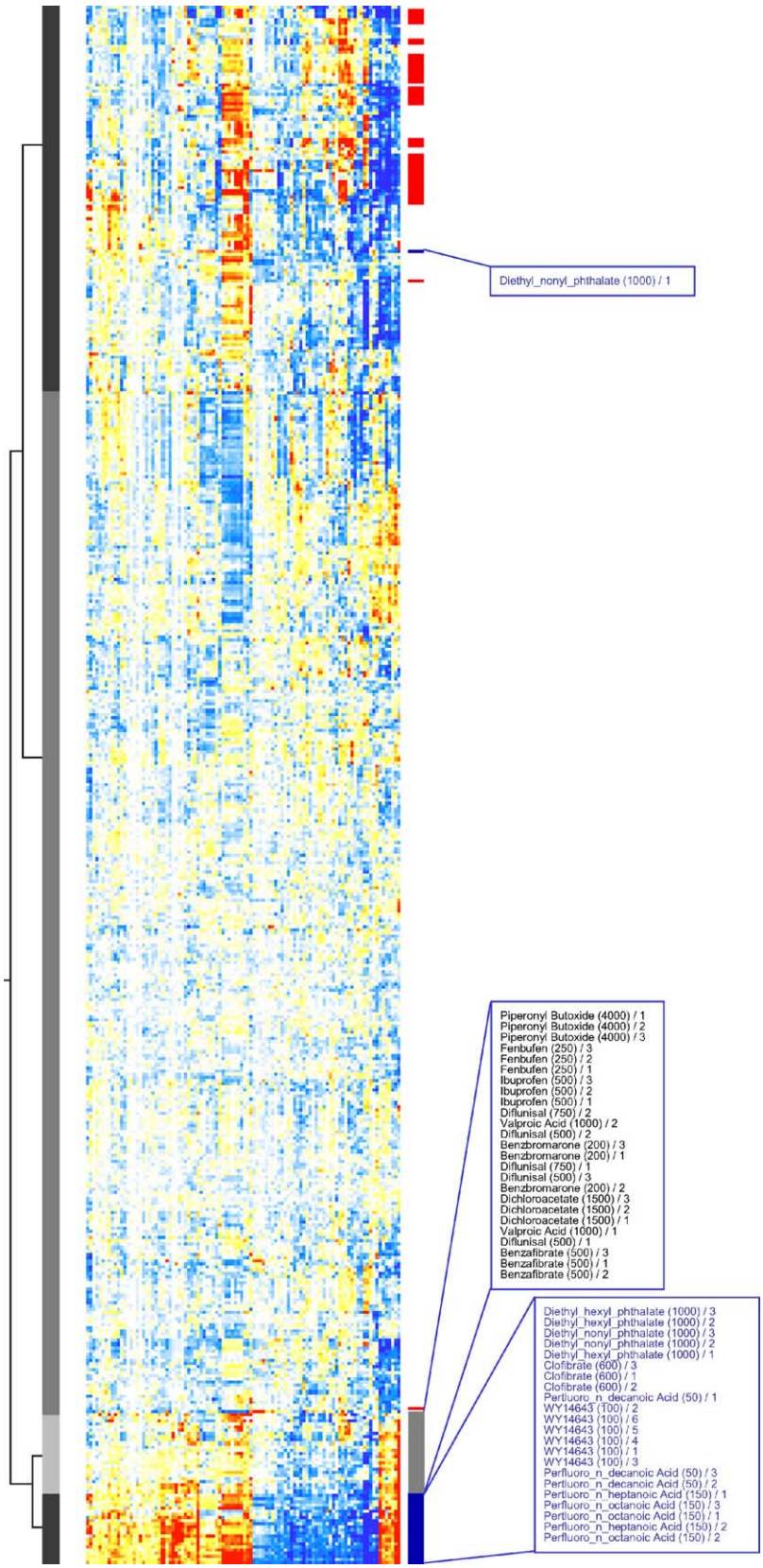

Fig. 5. A peroxisome proliferator gene signature pattern. Clofibrate (600 mg/kg), WY 14643 (100 mg/kg), perfluoro-decanoic acid (50 mg/kg), perfluoro-heptanoic acid (150 mg/kg), perfluoro-octanoic acid (150 mg/kg), diethylhexyl phthalate (1000 mg/kg) and diethylnonyl phthlate (1000 mg/kg) were chosen as peroxisome proliferator training set samples (blue) and the 100 clones (genes listed in Table 3) that statistically best separate this training set from all other samples were determined and used for clustering. All the training set samples (but one replicate) cluster together; a second distinct cluster (compounds listed in black) co-clusters with the peroxisome proliferators away from all other compounds. Red indicates >2.8-fold increases and blue indicates >2.8-fold decreases in expression. Note the generally opposite gene regulations by macrophage activators (red) and peroxisome proliferators (blue).

differentially regulated, and, with the multivariate gene selection approach, least redundant). Many of these signature genes have been previously associated with macrophage activation.

Stat3 is a cytokine-induced transcription factor that induces most acute phase proteins [29], including α2-macroglobulin (A2m), manganese superoxide dismutase (SOD2), heme oxygenase (Hmox1), fibrinogen, tissue inhibitor of metalloproteinase 1 (TIMP-1), hemopexin (Hpx), and Orosomucoid 1 (Orm). Signature genes representing a negative acute phase response include binding proteins for insulin-like growth factor [30] and retinol [31]. Transcription of most cytochrome P450s are repressed by macrophage activators [12,13] as are many metabolic pathway genes, such as aldehyde dehydrogenases, glucose-6-phoshatase, urea cycle enzymes [32] and enzymes involved with lipid metabolism, particularly those responsive to PPARα agonists.

There are several recent studies showing that PPAR agonists and inflammatory stimuli are physiological antagonists in many tissues, and our study extends the concept to include PPARα agonists and macrophage activators in rat liver. Although our data are restricted to gene expression at 24 h, there is considerable literature support for macrophage activators as anti-peroxisome proliferators in the liver. LPS treatment decreases the size and number of hepatic peroxisomes and changes their lipid composition; other organelles are unaffected by LPS [33,34]. LPS has long been known to inhibit lipid metabolism, in particular beta oxidation of fatty acids, a major PPARα-inducible pathway [35]. The coordinated gene changes suggest regulation at the level of transcriptional factors. Recent work has shown rapid, pronounced repression by LPS of lipid metabolism-regulating transcription factors, including PPARα and its heteromer partner RXR in rodent liver [36]. This repression of PPARα is observed at mRNA, protein, and activity levels, and likely explains the pronounced down-regulation of many hepatic genes by LPS. The converse situation wherein macrophage activator-induced genes are repressed by peroxisome proliferators probably also involves regulation at the transcription factor level. There is evidence for PPAR repression of inflammatory and acute phase responses through interference with NF-κB pathways [37–39]. Stat3 is another macrophage activator-responsive transcription factor that we observed to be down-regulated by peroxisome proliferators, at least at the mRNA level; others have noted PPAR-stimulated dephosphorylation of Stat3 and inhibition of this pathway [40]. Further study is required to substantiate that many of the observed gene changes are of physiological, pharmacological, or toxicological relevance.

The close association between responses to several NSAIDs—particularly flufenamic acid, diclofenac and flurbiprofen—and macrophage activators by microarray analysis was unexpected, but cytokine responses confirmed an LPS—like effect of these NSAIDs. This similarity probably resulted from endotoxin absorption following damage to the GI tract, as GI lesions were observed after high oral doses of almost all NSAIDs. Blood endotoxin levels were reported to be elevated in patients on high dose NSAID therapy [26]. There is also evidence in favor of gut-derived endotoxin involvement in hepatotoxicities of solvents such as carbon tetrachloride, dimethylnitrosamine, thioacetamide, and allyl alcohol [27,28]. Many NSAIDs also bind and activate or inhibit PPAR transcription factors [41]. Diflunisal (at two high doses) co-clustered with peroxisome proliferators in this study suggesting PPARα activity for this compound. Ibuprofen and fenbufen clustered with both macrophage activators and peroxisome proliferators, reflecting gene responses of both classes. Most other NSAIDs either clustered with macrophage activators alone, or cluster independently of these two toxicant classes. Diclofenac reportedly inhibits PPAR activity [41], and NSAIDs that inhibit PPARα and act oppositely to peroxisome proliferators would be expected to more closely resemble macrophage activators in their transcriptional responses.

Macrophage activators induce several chaperone proteins/ER stress proteins, such as Grp58 (also known as ER-60, Erp57 and HIP-70), calreticulin, and protein disulfide isomerase, which may reflect adaptive changes to cellular stress and damage. These are multifunctional, ER proteins that bind to one another, are important in nascent and damaged protein folding, have anti-oxidant and sulfhydryl group protector activity, and appear to be repressed by peroxisome proliferators [42]. The preferential association of these gene inductions with macrophage activators is somewhat surprising given the large number of hepatotoxicants in our database that produce reactive electrophiles and oxidative stress that would be expected to produce similar stress and damage. Other groups have provided evidence for macrophage activator regulation of this class of proteins: LPS increases expression of many of these multifunctional proteins [43,44], Grp58 associates with and may regulate the cytokine-responsive transcription factor Stat3 [45], and other transcription factors are involved in responses to macrophage activators. Cyclophilin B may even be a cytokine [46].

Gadolinium chloride, concanavalin A, and carbon tetrachloride are known to transiently activate Kupffer cells, and were the only co-clustered LPS-like compounds that did not induce multiple PCR markers of macrophage activation in our study. The lack of effects on cytokines may reflect the single 24 h time point that was used. Gadolinium chloride injection rapidly kills differentiated macrophages, releasing TNFα and other cytokines in the process [22,23], which may account for the similar gene expression pattern to LPS and zymosan A. Concanavalin A, a T lymphocyte activator, increased only IL-6 mRNA among our cytokine mRNA markers, but short-lived increases in interferon-γ, TNFα and iNOS have been associated with concanavalin A-induced hepatotoxicity [25,47]. The role of

Kupffer cells in carbon tetrachloride-induced hepatotoxicity in rodents is well established, with early increases in TNFα being an important contributor [19].

Several compounds reported to be macrophage activators—estrogen [48], Vitamin A [49], hexachlorocyclohexane γ (lindane) [50], and cadmium [51]—failed to co-cluster with LPS. These compounds may activate macrophages in a different manner from LPS, possibly with a more prolonged time course, or perhaps they have additional effects on hepatic gene expression that mask the effects of macrophage activation. However, none of these compounds increased cytokine RNA markers in the present study.

This study shows that gene expression data generated from microarrays can provide a means of identifying macrophage activation. Our goal is to identify gene signature profiles for as many different types of hepatotoxicity as possible using microarray gene expression data from the 100 or so paradigm compounds in Appendix A. To the extent that robust gene responses are initiated by 24 h and suitable training set compounds can be identified for other classes of hepatotoxicity, our 100 paradigm compound database will be useful in defining signature gene expression patterns that distinguish between a number of different hepatotoxicity classes.

The broad coverage of compounds utilized in the present study allows meaningful comparison and clustering across hepatotoxicant classes. While 'phenotypic anchoring' of microarray data to pathology data [7] is necessary for interpretation of effects of novel compounds, the 100 compounds employed in the present study and their pathologies are relatively well characterized. Some adverse effects (such as the NSAID effects on the GI tract) were noted at 24 h necropsy (Appendix A). Our microarray data largely confirmed published findings, and the novel associations of genes and compounds gleaned from the microarray data generally provided an interesting starting point for further study. Compromises on cost and number of samples and replicate microarrays were made. Similar compromises were made with the time course (only 24 h data was used, which resulted in the loss of time-shifted responses) and dose selection (in general a single high toxic dose was used). In those cases where multiple doses were given, generally only the highest dose was associated with LPS-like gene expression (e.g., most of the NSAIDs; Appendix A). Overall, the lower dose multiples for transcriptional profiling was disappointing. Microarray analysis with three independent biological samples greatly increased confidence in classification of results versus analysis with single pooled samples, and can be utilized to assess the performance of data analysis tools such as data normalization and clustering algorithms. Thus, the additional samples can be used to compare and distinguish between different approaches.

Genes that are common to multiple dissimilar selection approaches can be accepted with greater confidence than genes from any one gene selection approach alone. Similarly, compounds that co-cluster with a training set of compounds are more believable when co-clustering is observed regardless of the approach used to select the training gene set. Microarray-based studies that involve a single compound are becoming common in the literature [52,53]. These studies may yield high quality data about that compound, but extrapolating those gene changes to other compounds in that toxicological class is difficult and can be misleading. The broad coverage of compounds in the present study allows us to evaluate macrophage activators and peroxisome proliferators as classes of compounds rather than just LPS and clofibrate as individual toxicants; to the extent that the toxicant class members are similar, the increased number of compounds behave like increased replicates, increasing the power for analysis.

This study adds to an increasing body of evidence supporting the utility of gene transcriptional profiling for toxicity evaluation. Even with a relatively limited data set, robust shared profiles were found between compounds having similar modes of action, and these should be useful to facilitate the recognition of additional members of these compound classes. The use of this technology in toxicology seems certain to increase as the technology continues to improve and additional applications are demonstrated.

Acknowledgments

The support and guidance of Dr. William Powers and Dr. Michael Jackson is gratefully acknowledged. We thank Dr. Druie Cavender for comments and criticisms. We thank Dr. Ed Frizell for early approaches to the peroxisome proliferator data.

Appendix A. Hepatic RNA was obtained from male rats treated with the following compounds for 24 h

Compound	Route of administration	Dose (mg/kg)	Observations at or prior to necropsy
ANIT	Both	75 (i.p.), 50,200 (oral)	Highest oral dose; inactive, stomach food filled 3/3
Acetamidofluorene	Oral	200	
Allyl alcohol	Oral	125	Liver mottled, yellow (moderate) 2/3
Amiodarone	Oral	600, 1000	Highest dose; inactive, stomach food filled 3/3

Appendix A. (*Continued*)

Compound	Route of administration	Dose (mg/kg)	Observations at or prior to necropsy
Amsacrine	i.p.	20	
Aniline	Oral	200	
Antimycin A3	i.p.	2	
Aspirin	Oral	600	
Benzafibrate	Oral	500	
Benzbromarone	Oral	200	
Bromobenzene	Oral	900	
Buspirone	Oral	100	
Busulfan	i.p.	100	
Butylated hydroxytoluene	Oral	1000	Stomach food filled 3/3; kidneys mottled dark 3/3
Cadmium chloride	Oral	30, 75	Highest dose; GI tract fluid filled-moderate 1/3; kidneys both mottled-pale 1/3; stomach food filled 2/3
Captopril	Oral	5000	
Carbon tetrachloride	Oral	3200	Liver pale and moderately enlarged 5/6
Carmustine	Oral	30	
Cerium chloride	Oral	50	Kidney mottled/pale 1/3
Chlorambucil	Both	25 (i.p.), 60 (oral)	High oral dose; dry red exudate on face 1/3; inactive, stomach food filled 1/1
Cisplatin	Oral	25	Moderate hydronephrosis 1/3; kidney mottled and pale 1/3
Clofibrate	Oral	600	GI tract air filled-moderate 1/3
Concanavalin A	i.p.	20	
Coumarin	Oral	400	Prone, stomach food filled 6/6; liver mottled/dark grainy appearance 6/6; red urine 5/6; prostration and moderate salivation, buccal staining 6/6
Cyclophosphamide	Oral	40	
Dacarbazine	i.p.	200	
Dichloroacetate	Oral	1500	
Diclofenac	Oral	75	Slightly enlarged liver 3/3; dark contents of GI tract 3/3
Dieldrin	Oral	30, 45	
Diethyl_hexyl_phthalate	Oral	1000	Liver slightly enlarged 1/3
Diflunisal	Oral	500, 750	Highest dose; inactive, stomach food filled 3/3
Diiso_nonyl_phthlate	Oral	1000	Liver slightly enlarged 3/3
Dimethylformamide	i.p.	1000	
Dimethylmaleate	i.p.	400	
Dimethylnitrosamine	Oral	50	Liver dark and mottled, moderately enlarged 3/3
Disulfiram	Oral	2000	Inactive, white material in stomach 3/3
Doxorubicin	i.p.	20	
Erythromycin estolate	Oral	1500	Inactive, stomach food filled 3/3
Ethinyl estradiol	Oral	500	
Etoposide	Both	120 (i.p.), 150 (oral)	Intravenous dose; abdominal cavity-adhesions with white material present 3/3; cecum enlarged with gray contents 1/3
Famotidine	Oral	500	
Fenbufen	Oral	250	Dark contents of GI tract 6/6

Appendix A. (*Continued*)

Compound	Route of administration	Dose (mg/kg)	Observations at or prior to necropsy
Flufenamic acid	Oral	150, 250	Highest dose; dark contents of GI tract 3/3; cecum distended 1/3
Fluoxetine	Oral	50, 100	
Flurbiprofen	Oral	40	Dark contents of GI tract 2/3
Flutamide	Oral	500	Inactive, stomach food filled 6/6
Furosemide	Oral	1500	Inactive, stomach food filled 3/3; yellow/green contents in GI tract 2/3
Gadolinium	i.p.	300	Abdominal cavity-multiple adhesions with white superficial discoloration of most organ surfaces
Galactosamine	i.p.	3000	Liver moderately enlarged 2/3; mottled pale/dark 3/3
Gentamycin	i.p.	750	2 mm yellow focus on median lobe 1/3; spleen enlarged and pale 1/3
Glibenclamide	Oral	3000, 5010	
Glucosamine	i.p.	2000	
Glycine	i.p.	500	
Hexachlorocyclohexane	Oral	40, 65, 80	Highest dose; inactive, stomach food filled 3/3; kidneys mottled dark 1/3
Hydrazine hydrate	Oral	60	Inactive, stomach food filled 3/3; liver mottled/dark foci, slightly enlarged 3/3
Ibuprofen	Oral	500	Dark contents of GI tract 3/3
Indomethacin	i.p.	30	
Isoproterenol	i.p.	9	
LPS	i.p.	3, 10	
Menadione	Oral	250	
Metformin	Oral	750	
Methapyrilene	i.p.	100	
Methylcholanthrene	i.p.	150	
Methylenedianiline	Oral	100	
4-Methylthiazole	Oral	120	Kidneys mottled dark 1/4
Metoprolol	Oral	2000	
Monocrotaline	Oral	30	
Niacin USP XXIII	Oral	2505, 5010	Highest dose; inactive, stomach food filled 3/3
Nimesulide	Oral	500	Kidneys-interior darkened 3/3
Paraquat	Oral	100	Cecum filled with gray contents 1/3
Perfluoro_n_decanoic acid	Oral	50	
Perfluoro_n_heptanoic acid	Oral	150	
Perfluoro_n_octanoic acid	Oral	150	
Perhexilene	Oral	2000	
Phalloidin	i.p.	1	
Phenacetin	i.p.	1200	
Phenylephrine	i.p.	5	Kidney mottled and pale 2/4
Phorone	i.p.	500	
Picoline_n_oxide	Oral	200	
Piperonal	Oral	2000	Inactive, stomach food filled 3/3
Piperonyl butoxide	Oral	4000	Inactive, stomach food filled 3/3; urine staining 1/3
Precocene I	i.p.	500	Liver multiple white foci on lobes, stippling effect 3/3

Appendix A. (*Continued*)

Compound	Route of administration	Dose (mg/kg)	Observations at or prior to necropsy
Pregnenolone_16a_carbonitrile	Oral	200	
Pulegone	Oral	400	Inactive, stomach food filled 3/3; decreased activity 3/3
Puromycin	Oral	350	Kidneys mottled, dark 1/3
Quercetin	Oral	1995, 4005	Highest dose; kidneys mottled dark 1/3; GI tract-yellow contents
Rifampin	Oral	600	
Rotenone	Both	6 (i.p.), 4100 (oral)	Highest oral dose; inactive, stomach food filled 3/3
Sodium vanadate	i.p.	20	
Streptozocin	i.p.	138	
Sulindac	Oral	400	
Tacrine	Oral	50	Kidneys mottled dark 3/3; moderate salivation and urine staining 3/3 exopthalmia 1/3, chromodacryorrhea 2/3
Tannic acid	Oral	3000	Inactive, stomach food filled 3/3; kidneys mottled 1/3
Tetracycline	Both	600 (i.p.), 500 (oral)	Intravenous dose; adhesions in abdominal cavity; spleen pale, liver pale 1/3
Thioacetamide	Oral	70, 150	High dose; kidneys mottled dark 3/3
Trans anethole	i.p.	600	
Troglitazone	Oral	100, 500	High dose; kidneys clear foci 1/3
Valproic acid	Oral	200, 600,1000	
Vitamin A	Oral	100, 200	
WY 14643	Oral	100	
Zymosan A	i.p.	250	Inactive; GI tract moderately filled 3/3; spleen pale 2/3; white areas on liver 1/3

References

[1] Aardema MJ, MacGregor JT. Toxicology and genetic toxicology in the new era of "toxicogenomics": impact of "-omics" technologies. Mutat Res 2002;499(1):13–25.

[2] Pennie WD, Woodyatt NJ, Aldridge TC, Orphanides G. Application of genomics to the definition of the molecular basis for toxicity. Toxicol Lett 2001;120(1–3):353–8.

[3] Ulrich R, Friend SH. Toxicogenomics and drug discovery: will new technologies help us produce better drugs? Nat Rev Drug Discov 2002;1(1):84–8.

[4] Waring JF, Jolly RA, Ciurlionis R, Lum PY, Praestgaard JT, Morfitt DC, et al. Clustering of hepatotoxins based on mechanism of toxicity using gene expression profiles. Toxicol Appl Pharmacol 2001;175(1): 28–42.

[5] Bartosiewicz MJ, Jenkins D, Penn S, Emery J, Buckpitt A. Unique gene expression patterns in liver and kidney associated with exposure to chemical toxicants. J Pharmacol Exp Therapeut 2001;297(3): 895–905.

[6] Boorman GA, Anderson SP, Casey WM, Brown RH, Crosby LM, Gottschalk K, et al. Toxicogenomics, drug discovery, and the pathologist. Toxicol Pathol 2002;30(1):15–27.

[7] Hamadeh HK, Knight BL, Haugen AC, Sieber S, Amin RP, Bushel PR, et al. Methapyrilene toxicity: anchorage of pathologic observations to gene expression alterations. Toxicol Pathol 2002;30(4):470–82.

[8] Jaeschke H, Gores GJ, Cederbaum AI, Hinson JA, Pessayre D, Lemasters JJ. Mechanisms of hepatotoxicity. Toxicol Sci 2002;65(2): 166–76.

[9] Streetz KL, Wustefeld T, Klein C, Manns MP, Trautwein C. Mediators of inflammation and acute phase response in the liver. Cell Mol Biol 2001;47(4):661–73.

[10] Laskin JD, Heck DE, Gardner CR, Laskin DL. Prooxidant and antioxidant functions of nitric oxide in liver toxicity. Antioxid Redox Signal 2001;3(2):261–71.

[11] Dhainaut JF, Marin N, Mignon A, Vinsonneau C. Hepatic response to sepsis: interaction between coagulation and inflammatory processes. Crit Care Med 2001;29(7 Suppl):S42–7.

[12] Morgan ET. Regulation of cytochrome p450 by inflammatory mediators: why and how? Drug Metab Dispos 2001;29(3):207–12.

[13] Renton KW. Alteration of drug biotransformation and elimination during infection and inflammation. Pharmacol Therapeut 2001; 92(2/3):147–63.

[14] Hoshiya T, Watanabe D, Akagi K, Mizoguchi Y, Kamiya K, Mizuguchi H, et al. Acute phase response in toxicity studies. I. Survey of beagle dogs subjected to single-dose toxicity studies. J Toxicol Sci 2001;26(2):95–102.

[15] Ricote M, Li AC, Willson TM, Kelly CJ, Glass CK. The peroxisome proliferator-activated receptor-gamma is a negative regulator of macrophage activation. Nature 1998;391(6662):79–82.

[16] Salunga RC, Guo H, Luo L, Bittner A, Joy KC, Chambers JR, et al. Gene expression analysis via cDNA microarrays of laser capture microdissected cells from fixed tissue. DNA Microarrays 1999: 121–37.
[17] Burczynski ME, McMillian M, Ciervo J, Li L, Parker JB, Dunn II RT, et al. Toxicogenomics-based discrimination of toxic mechanism in HepG2 human hepatoma cells. Toxicol Sci 2000;58(2):399–415.
[18] Przybocki JM, Reuhl KR, Thurman RG, Kauffman FC. Involvement of nonparenchymal cells in oxygen-dependent hepatic injury by allyl alcohol. Toxicol Appl Pharmacol 1992;115(1):57–63.
[19] Morio LA, Chiu H, Sprowles KA, Zhou P, Heck DE, Gordon MK, et al. Distinct roles of tumor necrosis factor-alpha and nitric oxide in acute liver injury induced by carbon tetrachloride in mice. Toxicol Appl Pharmacol 2001;172(1):44–51.
[20] Horn TL, O'Brien TD, Schook LB, Rutherford MS. Acute hepatotoxicant exposure induces TNFR-mediated hepatic injury and cytokine/apoptotic gene expression. Toxicol Sci 2000;54(1):262–73.
[21] Stachlewitz RF, Seabra V, Bradford B, Bradham CA, Rusyn I, Germolec D, et al. Glycine and uridine prevent D-galactosamine hepatotoxicity in the rat: role of Kupffer cells. Hepatology 1999; 29(3):737–45.
[22] Rose ML, Bradford BU, Germolec DR, Lin M, Tsukamoto H, Thurman RG. Gadolinium chloride-induced hepatocyte proliferation is prevented by antibodies to tumor necrosis factor alpha. Toxicol Appl Pharmacol 2001;170(1):39–45.
[23] Ruttinger D, Vollmar B, Wanner GA, Messmer K. In vivo assessment of hepatic alterations following gadolinium chloride-induced Kupffer cell blockade. J Hepatol 1996;25(6):960–7.
[24] Andres D, Sanchez-Reus I, Bautista M, Cascales M. Depletion of Kupffer cell function by gadolinium chloride attenuates thioacetamide-induced hepatotoxicity: expression of metallothionein and HSP70. Biochem Pharmacol 2003;66(6):917–26.
[25] Mizuhara H, O'Neill E, Seki N, Ogawa T, Kusunoki C, Otsuka K, et al. T cell activation-associated hepatic injury: mediation by tumor necrosis factors and protection by interleukin 6. J Exp Med 1994;179(5):1529–37.
[26] Busch J, Hammer M, Brunkhorst R, Wagener P. Determination of endotoxin in inflammatory rheumatic diseases—the effect of non-steroidal anti-inflammatory agents on intestinal permeability. Zeitschrift Rheumatol 1988;47(3):156–60.
[27] Plummer JL, Ossowicz CJ, Whibley C, Ilsley AH, Hall PD. Influence of intestinal flora on the development of fibrosis and cirrhosis in a rat model. J Gastroenterol Hepatol 2000;15(11):1307–11.
[28] Roth RA, Harkema JR, Pestka JP, Ganey PE. Is exposure to bacterial endotoxin a determinant of susceptibility to intoxication from xenobiotic agents? Toxicol Appl Pharmacol 1997;147(2):300–11.
[29] Andrejko KM, Chen J, Deutschman CS. Intrahepatic STAT-3 activation and acute phase gene expression predict outcome after CLP sepsis in the rat. Am J Physiol 1998;275(6 Pt 1):G1423–9.
[30] Priego T, De II C, Martin AI, Villanua MA, Lopez-Calderon A. Hepatic insulin-like growth factor-I binding protein 3 gene expression in rats with endotoxic shock: the role of glucocorticoids. Ann N Y Acad Sci 2002;973:88–90.
[31] Rosales FJ, Ross AC. A low molar ratio of retinol binding protein to transthyretin indicates vitamin A deficiency during inflammation: studies in rats and a posterior analysis of vitamin A-supplemented children with measles. J Nutr 1998;128(10):1681–7.
[32] Tabuchi S, Gotoh T, Miyanaka K, Tomita K, Mori M. Regulation of genes for inducible nitric oxide synthase and urea cycle enzymes in rat liver in endotoxin shock. Biochem Biophys Res Commun 2000; 268(1):221–4.
[33] Contreras MA, Khan M, Smith BT, Cimini AM, Gilg AG, Orak J, et al. Endotoxin induces structure-function alterations of rat liver peroxisomes: Kupffer cells released factors as possible modulators. Hepatology 2000;31(2):446–55.
[34] Khan M, Contreras M, Singh I. Endotoxin-induced alterations of lipid and fatty acid compositions in rat liver peroxisomes. J Endotoxin Res 2000;6(1):41–50.
[35] Hardardottir I, Grunfeld C, Feingold KR. Effects of endotoxin on lipid metabolism. Biochem Soc Trans 1995;23(4):1013–8.
[36] Beigneux AP, Moser AH, Shigenaga JK, Grunfeld C, Feingold KR. The acute phase response is associated with retinoid X receptor repression in rodent liver. J Biol Chem 2000;275(21):16390–9.
[37] Staels B, Koenig W, Habib A, Merval R, Lebret M, Torra IP, et al. Activation of human aortic smooth-muscle cells is inhibited by PPARalpha but not by PPARgamma activators. Nature 1998; 393(6687):790–3.
[38] Dubuquoy L, Dharancy S, Nutten S, Pettersson S, Auwerx J, Desreumaux P. Role of peroxisome proliferator-activated receptor gamma and retinoid X receptor heterodimer in hepatogastroenterological diseases. Lancet 2002;360(9343):1410–8.
[39] Kleemann R, Gervois PP, Verschuren L, Staels B, Princen HM, Kooistra T. Fibrates down-regulate IL-1-stimulated C-reactive protein gene expression in hepatocytes by reducing nuclear p50-NFkappa B-C/EBP-beta complex formation. Blood 2003;101(2): 545–51.
[40] Takata Y, Kitami Y, Yang ZH, Nakamura M, Okura T, Hiwada K. Vascular inflammation is negatively autoregulated by interaction between CCAAT/enhancer-binding protein-delta and peroxisome proliferator-activated receptor-gamma. Circ Res 2002;91(5):427–33.
[41] Adamson DJ, Frew D, Tatoud R, Wolf CR, Palmer CN. Diclofenac antagonizes peroxisome proliferator-activated receptor-gamma signaling. Mol Pharmacol 2002;61(1):7–12.
[42] Muhlenkamp CR, Gill SS. A glucose-regulated protein, GRP58, is down-regulated in C57B6 mouse liver after diethylhexyl phthalate exposure. Toxicol Appl Pharmacol 1998;148(1):101–8.
[43] Ejima K, Layne MD, Carvajal IM, Nanri H, Ith B, Yet SF, et al. Modulation of the thioredoxin system during inflammatory responses and its effect on heme oxygenase-1 expression. Antioxid Redox Signal 2002;4(4):569–75.
[44] Huang YH, Chang AY, Huang CM, Huang SW, Chan SH. Proteomic analysis of lipopolysaccharide-induced apoptosis in PC12 cells. Proteomics 2002;2(9):1220–8.
[45] Guo GG, Patel K, Kumar V, Shah M, Fried VA, Etlinger JD, et al. Association of the chaperone glucose-regulated protein 58 (GRP58/ER-60/ERp57) with Stat3 in cytosol and plasma membrane complexes. J Interferon Cytokine Res 2002;22(5):555–63.
[46] Billich A, Winkler G, Aschauer H, Rot A, Peichl P. Presence of cyclophilin A in synovial fluids of patients with rheumatoid arthritis. J Exp Med 1997;185(5):975–80.
[47] Gantner F, Leist M, Lohse AW, Germann PG, Tiegs G. Concanavalin A-induced T-cell-mediated hepatic injury in mice: the role of tumor necrosis factor. Hepatology 1995;21(1):190–8.
[48] Ikejima K, Enomoto N, Iimuro Y, Ikejima A, Fang D, Xu J, et al. Estrogen increases sensitivity of hepatic Kupffer cells to endotoxin. Am J Physiol 1998;274(4 Pt 1):G669–76.
[49] Wueweera JB, Gandolfi AJ, Badger DA, Sipes IG, Brendel K. Vitamin A potentiation of vinylidene chloride hepatotoxicity in rats and precision-cut rat liver slices. Fundam Appl Toxicol 1996;34(1): 73–83.
[50] Videla LA, Troncoso P, Arisi AC, Junqueira VB. Dose-dependent effects of acute lindane treatment on Kupffer cell function assessed in the isolated perfused rat liver. Xenobiotica 1997;27(7):747–57.
[51] Sauer JM, Waalkes MP, Hooser SB, Kuester RK, McQueen CA, Sipes IG. Suppression of Kupffer cell function prevents cadmium induced hepatocellular necrosis in the male Sprague–Dawley rat. Toxicology 1997;121(2):155–64.
[52] Dong H, Toyoda N, Yoneyama H, Kurachi M, Kasahara T, Kobayashi Y, et al. Gene expression profile analysis of the mouse liver during bacteria-induced fulminant hepatitis by a cDNA microarray system. Biochem Biophys Res Commun 2002;298(5):675–86.

[53] Liu J, Saavedra JE, Lu T, Song JG, Clark J, Waalkes MP, et al. *O*(2)-Vinyl 1-(pyrrolidin-1-yl)diazen-1-ium-1,2-diolate protection against D-galactosamine/endotoxin-induced hepatotoxicity in mice: genomic analysis using microarrays. J Pharmacol Exp Therapeut 2002;300(1): 18–25.

[54] Mitani K, Fujita H, Kappas A, Sassa S. Heme oxygenase is a positive acute-phase reactant in human Hep3B hepatoma cells. Blood 1992; 79(5):1255–9.

[55] Rizzardini M, Terao M, Falciani F, Cantoni L. Cytokine induction of haem oxygenase mRNA in mouse liver. Interleukin 1 transcriptionally activates the haem oxygenase gene. Biochem J 1993;290(Pt 2):343–7.

[56] Roeb E, Graeve L, Mullberg J, Matern S, Rose-John S. TIMP-1 protein expression is stimulated by IL-1 beta and IL-6 in primary rat hepatocytes. FEBS Lett 1994;349(1):45–9.

[57] Ogata I, Auster AS, Matsui A, Greenwel P, Geerts A, D'Amico T, et al. Up-regulation of type I procollagen C-proteinase enhancer protein messenger RNA in rats with CCl4-induced liver fibrosis. Hepatology 1997;26(3):611–7.

[58] Banyai L, Patthy L. The NTR module: domains of netrins, secreted frizzled related proteins, and type I procollagen C-proteinase enhancer protein are homologous with tissue inhibitors of metalloproteases. Prot Sci 1999;8(8):1636–42.

[59] Dougall WC, Nick HS. Manganese superoxide dismutase: a hepatic acute phase protein regulated by interleukin-6 and glucocorticoids. Endocrinology 1991;129(5):2376–84.

[60] Tolosano E, Altruda F. Hemopexin: structure, function, and regulation. DNA Cell Biol 2002;21(4):297–306.

[61] Milosavljevic TS, Petrovic MV, Cvetkovic ID, Grigorov II. DNA binding activity of C/EBPbeta and C/EBPdelta for the rat alpha2-macroglobulin gene promoter is regulated in an acute-phase dependent manner. Biochem Russ 2002;67(8):918–26.

[62] Ryckman C, Vandal K, Rouleau P, Talbot M, Tessier PA. Proinflammatory activities of S100: proteins S100A8, S100A9, and S100A8/A9 induce neutrophil chemotaxis and adhesion. J Immunol 2003;170(6):3233–42.

[63] Zhao F, Yuan Q, Sultzer BM, Chung SW, Wong PM. The involvement of Ran GTPase in lipopolysaccharide endotoxin-induced responses. J Endotoxin Res 2001;7(1):53–6.

[64] Spolarics Z. Endotoxemia, pentose cycle, and the oxidant/antioxidant balance in the hepatic sinusoid. J Leukoc Biol 1998;63(5):534–41.

[65] Takuwa Y, Takuwa N, Sugimoto N. The Edg family G protein-coupled receptors for lysophospholipids: their signaling properties and biological activities. J Biochem 2002;131(6):767–71.

[66] Meier B. Superoxide generation of phagocytes and nonphagocytic cells. Protoplasma 2001;217(1–3):117–24.

[67] Dax CI, Lottspeich F, Mullner S. In vitro model system for the identification and characterization of proteins involved in inflammatory processes. Electrophoresis 1998;19(10):1841–7.

[68] Guicciardi ME, Miyoshi H, Bronk SF, Gores GJ. Cathepsin B knockout mice are resistant to tumor necrosis factor-alpha-mediated hepatocyte apoptosis and liver injury: implications for therapeutic applications. Am J Pathol 2001;159(6):2045–54.

[69] Smith SM, Snyder IS. Effect of lipopolysaccharide and lipid A on mouse liver pyruvate kinase activity. Infect Immun 1975;12(5): 993–8.

[70] Morgan ET, Li-Masters T, Cheng PY. Mechanisms of cytochrome P450 regulation by inflammatory mediators. Toxicology 2002;181/182:207–10.

[71] Park CS, Baek HM, Chung WG, Lee KH, Ryu SD, Cha YN. Suppression of flavin-containing monooxygenase by overproduced nitric oxide in rat liver. Mol Pharmacol 1999;56(3):507–14.

[72] Satriano J, Schwartz D, Ishizuka S, Lortie MJ, Thomson SC, Gabbai F, et al. Suppression of inducible nitric oxide generation by agmatine aldehyde: beneficial effects in sepsis. J Cell Physiol 2001;188(3): 313–20.

[73] Bazel S, Andrejko KM, Chen J, Deutschman CS. Hepatic gene expression and cytokine responses to sterile inflammation: comparison with cecal ligation and puncture sepsis in the rat. Shock 1999;11(5):347–55.

[74] Maitra SR, Gestring ML, El-Maghrabi MR, Lang CH, Henry MC. Endotoxin-induced alterations in hepatic glucose-6-phosphatase activity and gene expression. Mol Cell Biochem 1999;196(1/2):79–83.

[75] Boustead JN, Stadelmaier BT, Eeds AM, Wiebe PO, Svitek CA, Oeser JK, et al. Hepatocyte nuclear factor-4 alpha mediates the stimulatory effect of peroxisome proliferator-activated receptor gamma co-activator-1 alpha (PGC-1 alpha) on glucose-6-phosphatase catalytic subunit gene transcription in H4IIE cells. Biochem J 2003;369(Pt 1):17–22.

[76] Morgan ET. Suppression of constitutive cytochrome P-450 gene expression in livers of rats undergoing an acute phase response to endotoxin. Mol Pharmacol 1989;36(5):699–707.

[77] Utili R, Abernathy CO, Zimmerman HJ. Inhibition of Na^+, K^+-adenosinetriphosphatase by endotoxin: a possible mechanism for endotoxin-induced cholestasis. J Infect Dis 1977;136(4):583–7.

[78] Bergad PL, Schwarzenberg SJ, Humbert JT, Morrison M, Amarasinghe S, Towle HC, et al. Inhibition of growth hormone action in models of inflammation. Am J Physiol Cell Physiol 2000;279(6): C1906–17.

[79] Maccarrone M, De Petrocellis L, Bari M, Fezza F, Salvati S, Di Marzo V, et al. Lipopolysaccharide downregulates fatty acid amide hydrolase expression and increases anandamide levels in human peripheral lymphocytes. Arch Biochem Biophys 2001;393(2):321–8.

[80] Beltowski J, Wojcicka G, Mydlarczyk M, Jamroz A. The effect of peroxisome proliferator-activated receptors alpha (PPARalpha) agonist, fenofibrate, on lipid peroxidation, total antioxidant capacity, and plasma paraoxonase 1 (PON 1) activity. J Physiol Pharmacol 2002; 53(3):463–75.

[81] Corton JC, Bocos C, Moreno ES, Merritt A, Marsman DS, Sausen PJ, et al. Rat 17 beta-hydroxysteroid dehydrogenase type IV is a novel peroxisome proliferator-inducible gene. Mol Pharmacol 1996;50(5): 1157–66.

[82] Foliot A, Touchard D, Mallet L. Inhibition of liver glutathione *S*-transferase activity in rats by hypolipidemic drugs related or unrelated to clofibrate. Biochem Pharmacol 1986;35(10):1685–90.

[83] Fayos BE, Bartles JR. Regulation of hepatocytic glycoprotein sialylation and sialyltransferases by peroxisome proliferators. J Biol Chem 1994;269(3):2151–7.

[84] Hakkola EH, Hiltunen JK, Autio-Harmainen HI. Mitochondrial 2,4-dienoyl-CoA reductases in the rat: differential responses to clofibrate treatment. J Lipid Res 1994;35(10):1820–8.

[85] Aoyama T, Peters JM, Iritani N, Nakajima T, Furihata K, Hashimoto T, et al. Altered constitutive expression of fatty acid-metabolizing enzymes in mice lacking the peroxisome proliferator-activated receptor alpha (PPARalpha). J Biol Chem 1998;273(10):5678–84.

[86] Ashour MB, Moody DE, Hammock BD. Apparent induction of microsomal carboxylesterase activities in tissues of clofibrate-fed mice and rats. Toxicol Appl Pharmacol 1987;89(3):361–9.

[87] Furihata T, Hosokawa M, Nakata F, Satoh T, Chiba K. Purification, molecular cloning, and functional expression of inducible liver acylcarnitine hydrolase in C57BL/6 mouse, belonging to the carboxylesterase multigene family. Arch Biochem Biophys 2003;416(1): 101–9.

[88] Hegardt FG. Mitochondrial 3-hydroxy-3-methylglutaryl-CoA synthase: a control enzyme in ketogenesis. Biochem J 1999;338(Pt 3):569–82.

[89] Cook L, Nagi MN, Piscatelli J, Joseph T, Prasad MR, Ghesquier D, et al. Hepatic subcellular distribution of short-chain beta-ketoacyl coenzyme A reductase and *trans*-2-enoyl coenzyme A hydratase: 25- to 50-fold stimulation of microsomal activities by the peroxisome proliferator, di-(2-ethylhexyl)phthalate. Arch Biochem Biophys 1986;245(1):24–36.

[90] Anderson NL, Esquer-Blasco R, Richardson F, Foxworthy P, Eacho P. The effects of peroxisome proliferators on protein abundances in mouse liver. Toxicol Appl Pharmacol 1996;137(1):75–89.

[91] Motojima K, Passilly P, Peters JM, Gonzalez FJ, Latruffe N. Expression of putative fatty acid transporter genes are regulated by peroxisome proliferator-activated receptor alpha and gamma activators in a tissue- and inducer-specific manner. J Biol Chem 1998; 273(27):16710–4.

[92] Giometti CS, Liang X, Tollaksen SL, Wall DB, Lubman DM, Subbarao V, et al. Mouse liver selenium-binding protein decreased in abundance by peroxisome proliferators. Electrophoresis 2000; 21(11):2162–9.

[93] Fischer M, You M, Matsumoto M, Crabb DW. Peroxisome proliferator-activated receptor alpha (PPARalpha) agonist treatment reverses PPARalpha dysfunction and abnormalities in hepatic lipid metabolism in ethanol-fed mice. J Biol Chem 2003;278(30):27997–8004.

[94] el Kebbaj MH, Cherkaoui Malki M, Latruffe N. Effect of peroxisomes proliferators and hypolipemic agents on mitochondrial inner membrane linked D-3-hydroxybutyrate dehydrogenase (BDH). Biochem Mol Biol Int 1995;35(1):65–77.

[95] Thomas H, Schladt L, Knehr M, Post K, Oesch F, Boiteux-Antoine AF, et al. Effect of hypolipidemic compounds on lauric acid hydroxylation and phase II enzymes. Biochem Pharmacol 1989;38(12): 1963–9.

[96] Motojima K, Isaka M, Takino Y, Goto S. Transient induction of fatty acid synthase in rat liver after removal of a peroxisome proliferator. FEBS Lett 1994;356(1):122–4.

[97] Kelleher DJ, Kreibich G, Gilmore R. Oligosaccharyltransferase activity is associated with a protein complex composed of ribophorins I and II and a 48 kDa protein. Cell 1992;69(1):55–65.

[98] Kumar V, Heinemann FS, Ozols J. Interleukin-2 induces *N*-glycosylation in T-cells: characterization of human lymphocyte oligosaccharyltransferase. Biochem Biophys Res Commun 1998;247(2): 524–9.

[99] Smith T, Ferreira LR, Hebert C, Norris K, Sauk JJ. Hsp47 and cyclophilin B traverse the endoplasmic reticulum with procollagen into pre-Golgi intermediate vesicles. A role for Hsp47 and cyclophilin B in the export of procollagen from the endoplasmic reticulum. J Biol Chem 1995;270(31):18323–8.

[100] Michalak M, Robert Parker JM, Opas M. Ca(2+) signaling and calcium binding chaperones of the endoplasmic reticulum. Cell Calcium 2002;32(5/6):269–78.

[101] Hannappel E, Huff T. The thymosins. Prothymosin alpha, parathymosin, and beta-thymosins: structure and function. Vitam Horm 2003;66:257–96.